VISUAL RESPONSE PROPERTIES OF NEURONS IN EXTRASTRIATE CORTEX OF THE OWL MONKEY

Thesis by

Steven Elery Petersen

In Partial Fulfillment of the Requirements

For the Degree of

Doctor of Philosophy

California Institute of Technology

Pasadena, California

1982

(Submitted August 26, 1981)

ACKNOWLEDGEMENTS

In five years of graduate school, a student builds up a long list of people who in some way have helped him along. I am no exception. I would especially wish to thank John Allman, my advisor, for several years of support, both intellectually and emotionally. Many thanks also to Jim Baker, my constant collaborator, for lending his expertise, experience and humor during experimental sessions, whether productive or frustrating. These two scientists provided me with an atmosphere where the research could be productive and fun. I wish to express my appreciation to Bill Newsome for his efforts in collaboration in Chapter 1 of my thesis. I am particularly indebted to Fran Miezin (Meizin, Miez Vin?) for his technical expertise, his patience, and his friendship, and to Bill Lease for his amazing ability to drive without looking.

I am grateful for the healthy moments of insanity afforded me by the men of the famous (notorious?) Caltech Biology fast pitch team. Good feelings and memories of these people, particularly Jim McCasland, Bob Murphy, and Dave Fink will be a comfort in my later years, when I am expected to, but probably will not, act more mature.

I am most grateful to my wife Bonnie, without whose constant support, trust and encouragement, I would not have made it to the stage of writing this page. She was a tower of strength, in good times and bad, and my appreciation for her patience with this temperamental biologist knows no bounds. I would also like to thank my parents for everything they have given, including forebearance to stick with a son who has spent 22 of his years in school. I also appreciate the support of my mother- and father-in-law for all they have done.

I would also like to acknowledge the assistance of countless people of the Biology Staff, especially Nancy Gill and Chris Vasquez-Balber, for making Beckman a better place to live, and for dispensing vast sums of money, and Connie Katz and Susan Mangrum for their aid in the preparation of my thesis.

Many thanks to Rae and Len Bergum for being our surrogate parents in California. I would like to thank Leslie Wolcott for the preparation of many of the figures in my thesis, and all the people at Graphic Arts for the many hours of work they put in to help me finish this thing off. Finally, I express my appreciation for the various funding agencies for their financial support including NIH Grants T32-GM07737, NS00178, NS-12131, NSF Grant BNS-77-15605, the Pew Memorial Trust, and the Weigle Memorial Fund.

ABSTRACT

The neurophysiological response properties of single neurons were studied quantitatively in four extrastriate areas of the owl monkey: the medial (M), dorsomedial (DM), dorsolateral (DL), and the middle temporal (MT) areas. Directionality was computed by comparing the responses to stimuli moved in the optimal and opposing directions; MT cells had much higher directionality to moving bars than cells in the other areas. Cells in all four areas were sharply tuned to the orientation of stationary flashed bars. Tuning for moving bars was broader than for flashed bars; DM cells were more sharply tuned to moving bars than were cells in the other areas. Tuning was broader to spots than to bars, while directionality was relatively unaffected. A moving array of random dots was the best stimulus for many MT neurons. Random dot stimuli were also effective in M, but evoked weak or no response from DM and DL cells. Extrastriate receptive fields were much larger than striate receptive fields. Eccentricity was correlated with receptive field size, but was uncorrelated with other variables.

Neurons in these four areas were tested for their selectivity to the spatial dimensions, the length and width, of visual stimuli. Cells in DL were much more selective for the spatial dimension than were cells in the other areas. The dimensional selectivity of DL cells is independent of the amount or sign of contrast in the receptive field, and the position of the stimulus within the receptive field. The optimal lengths and widths of visual stimuli are specified independently, and have a wide range of optimal dimensions from 1 to 30° in length, and from 0.25 to 7° in width.

Since many of the neurons of MT show strong directionality, it has been hypothesized that MT contributes to the perception of motion. A well-known aspect of motion perception is the phenomenon of direction-specific adaptation. We tested the neurons of MT for changes in responsiveness due to prolonged adaptation to stimuli

moving in various directions. For directional cells, the response to a bar was suppressed following adaptation in the best direction, and enhanced following adaptation in the opposite direction, when compared to the response to a bar following a period of stationary stimulation. For nondirection cells, the effects were much weaker, or absent.

These results support the notion of a localization of function among the various extrastriate areas.

Table of Contents

INTRODUCTION

The idea of cerebral localization of function received its first wide publicity and first serious setback in the middle of the 19th century when Gall and Spurzheim advanced the notion of cranioscopy or phrenology. Gall believed that specific regions of the cerebrum were responsible for such human qualitites as avarice and appreciation of music, and claimed that the development of these qualities could be discerned from bumps on the skull overlying the hyperthrophied cerebral regions. These beliefs have not withstood the test of empirical observation.

A major discovery that legitimized the notion of cerebral localization of function was reported by Fritsch and Hitsig in 1870 (10). They applied weak electrical stimulation to the exposed cerebral cortex of the dog and found that small movements of the animal's body could be elicited by stimulation of the precentral area of the cortex. Fritsch and Hitsig's results had three important implications. First, the cerebral cortex was shown to be excitable, which was contrary to the beliefs of the time. Second, in contradiction to Fluoren's accepted preachings on the functional equivalence of all cortex, the fact that weak electrical stimulation caused movements only when applied to the precentral cortex was a clear example of localization of function. Finally, the muscles which reacted to the stimulation were arranged in a topographic manner, with the facial muscles being represented most laterally, and the posterior limbs being represented more medially.

The repeatability and clarity of Fritsch and Hitsig's results and their interpretation of these results in light of the notion of functional localization were buttressed by the experiments and observations of many other workers. Slightly before the work of Fritsch and Hitsig, clinical observations by Broca implicated damage to a certain region of the frontal lobe of humans with particular disorders of speech production. Brodmann, through careful inspection of cortical cytoarchitecture, was able to delimit dozens of distinct subdivisions. Clinical studies by Holmes and anatomical

Figure 1. A schematic unfolding of the visual cortex of the left hemisphere in the owl monkey. The visual cortex corresponds to approximately the posterior third of the entire neocortex. The unfolded visual cortex is approximately a hemispherical surface, which is viewed from above in this diagram. The perimeter chart on the left shows the contralateral (right) half of the visual field. Abbreviations and conventions as in Figure 1, Chapter 1.

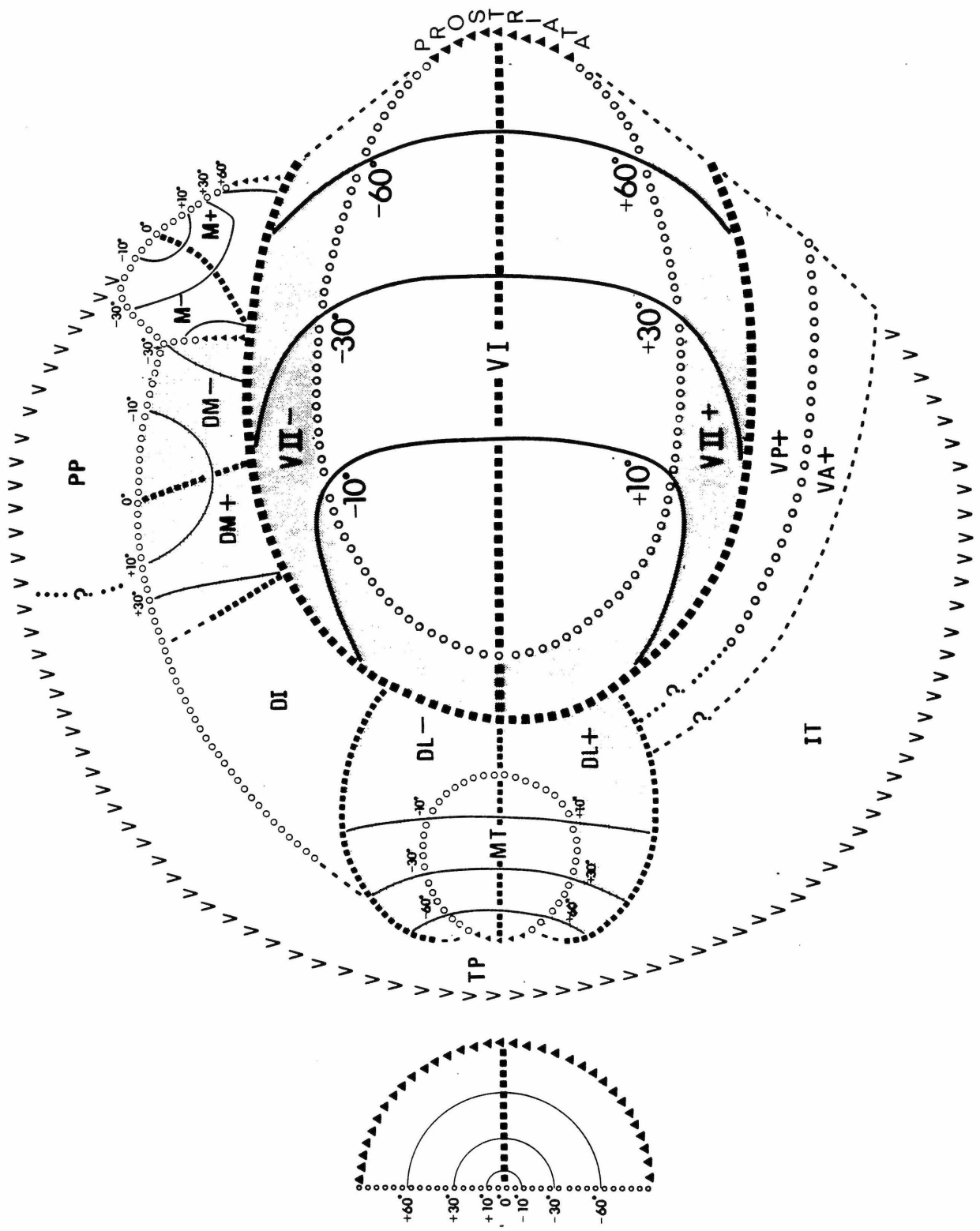
PROSTRIATA
-60°
+60°
-30°
+30°
-10°
+10°
VI
VII−
VII+
M+
M−
DM−
DM+
PP
DI
DL−
DL+
MT
VP+
VA+
IT
TP
?
+60°
+30°
+10°
0°
-10°
-30°
-60°

studies by many workers succeeded in localizing visual function to the occipital lobes and showing that there was also a topographic representation of visual space on the striate cortex such that nearby points in the field of vision are represented nearby on the striate map (see refs. 9,23).

The discovery of the topographic representation of sensory domains on cerebral cortex underlies another method of addressing the question of functional localization: the method of functional mapping. In the early 1940s, Lord Adrian, using evoked potential and implanted electrode techniques, described the representation of the skin on somatosensory cortex of several animals including pig, the shetland pony, and the ferret (1, 2). Woolsey recorded evoked potentials from small regions of the brains of anesthetized animals, while presenting the animals with somesthetic (30) or auditory stimuli (31). In this way he was able to map the animal's body onto the somatosensory cortex (SI) in monkey in regions 3A, 3B, 1, and 2, and to localize a second representation to the body (SII) in adjacent cortex. Likewise, the peripheral structure of the auditory system, the cochlea, which is organized in a tonotopic way (a representation of the domain of the frequency of sound waves), was mapped onto a region of the temporal lobe in two discrete representations.

Talbot, Marshall and Ades (16, 25) employed similar techniques in the study of the occipital lobe. Using visual stimulation, they found, not surprisingly, two representations of the visual hemifield in occipital cortex, and more laterally, a third region of visually responsive cortex. This lateral region has since become known as the Clare-Bishop area, after Clare and Bishop who were to rediscover it.

At this time, around 1950, circumscribed regions of cortex were thought to be contributing to particular sensory processes, while other areas were concerned with control of motor activity. These regions of known topographic cortex included about 30% of the cerebral cortex, with the remainder of cortex being deemed "association cortex," tissue in which higher order processing and interrelation of sensory information was thought to occur.

The single unit studies of Hubel and Wiesel on areas 17, 18, 19 (12, 13), made it clear that much could be learned not only about the response properties of cortical neurons, but also about the topographic representation of receptive field positions. In 1968, Allman and Kaas (3-8) began a series of microelectrode mapping studies of the topographic representation of visual space on the striate and adjoining cortex of the owl monkey. They found, much to their surprise, that owl monkey visual cortex is not aligned in three concentric belts, as in the cat, but that cortex beyond the second concentric region, V-II, consists of at least 7 visuotopically organized representations of all or part of the visual hemifield. These representations comprised approximately half of the cortex, and were complexly aligned so that there was minimal distortion of the visual representation at the borders of areas (see Fig. 1.).

Microelectrode mapping of the visual cortex of the cat was subsequently carried out by Tusa, Rosenquist, and Palmer (22, 26, 27). In cat visual cortex, there were found to be 13 visuotopic representations, again taking up a large percentage of cortex. Recent work on the visual cortex of the macaque (11, 19, 28, 29) has revealed a complex mosaic of areas as well. In other modalities, careful microelectrode mapping again led to the discovery of multiple representations. The region of somatosensory cortex formerly thought to contain a single representation, was shown to contain four representations of the skin (15, 17). In auditory cortex, tonotopic representations number at least four in the owl monkey (14) and the cat (see ref. 20), with six representations in macaque monkey auditory cortex (19). Motor and premotor cortex of the macaque has been shown to contain several representations of the face and hand (18, 23).

As can be seen in Fig. 1 in Chapter 1, the cortex of the owl monkey is now known to be populated in great part by topographic representations of the various modalities. The ubiquitous nature of these multiple representations has led to several lines of thought as to their significance. Hubel and Wiesel, because of the increasing

level of complexity of the neurons when moving from V1 to V2 to V3 (13), tentatively forwarded a hierarchical model for visual information processing. Merzenich and Kaas (20) have recently forwarded a different view as more data have been collected. They believe that there is a multiplicity of parallel channels which are complexly interconnected (see Fig. 2). Evidence at the present time seems to favor this view.

In the visual system of the owl monkey, the large number of visuotopic representations and the large amount of cortex devoted to these representations has led to the hypothesis that there is a localization of function to the various areas of visual perceptual abilities, or aspects of visuomotor coordination. To test this hypothesis, my collaborators and I began an assessment of the differences and similarities of four of the extrastriate areas of the owl monkey. We tested single unit properties in these four areas quantitatively for their responsiveness to simple visual stimuli, such as bars, spots, and fields of random dots, moving in different directions at different speeds, and in varying orientations. The similarities and differences between populations of cells from each of the four areas are reported in Chapter 1. Single unit studies of stimulus length, width, and diameter showed that one area, DL, had many cells that were particularly sensitive to the spatial dimensions of visual stimuli, while the other three areas tested did not. We then examined the dimensional selectivity of DL cells while varying the contrast or intensity of the stimulus, or the position of the stimulus within its excitatory receptive field. These results are reported in Chapter 2. The directional selectivity of many cells in MT led us to test MT cells for direction-specific adaptation. Direction-specific adaptation is one of a class of effects of prolonged adaptation to movement, which includes the classic waterfall illusion. The results of these experiments are reported in Chapter 3.

The outcome of studies of the physiological response properties of owl monkey extrastriate cells is strong evidence for functional localization in these areas.

Figure 2. Simplified wiring diagram of two pathways in owl monkey visual system. Conventions and abbreviations as in Figure 1, Chapter 1.

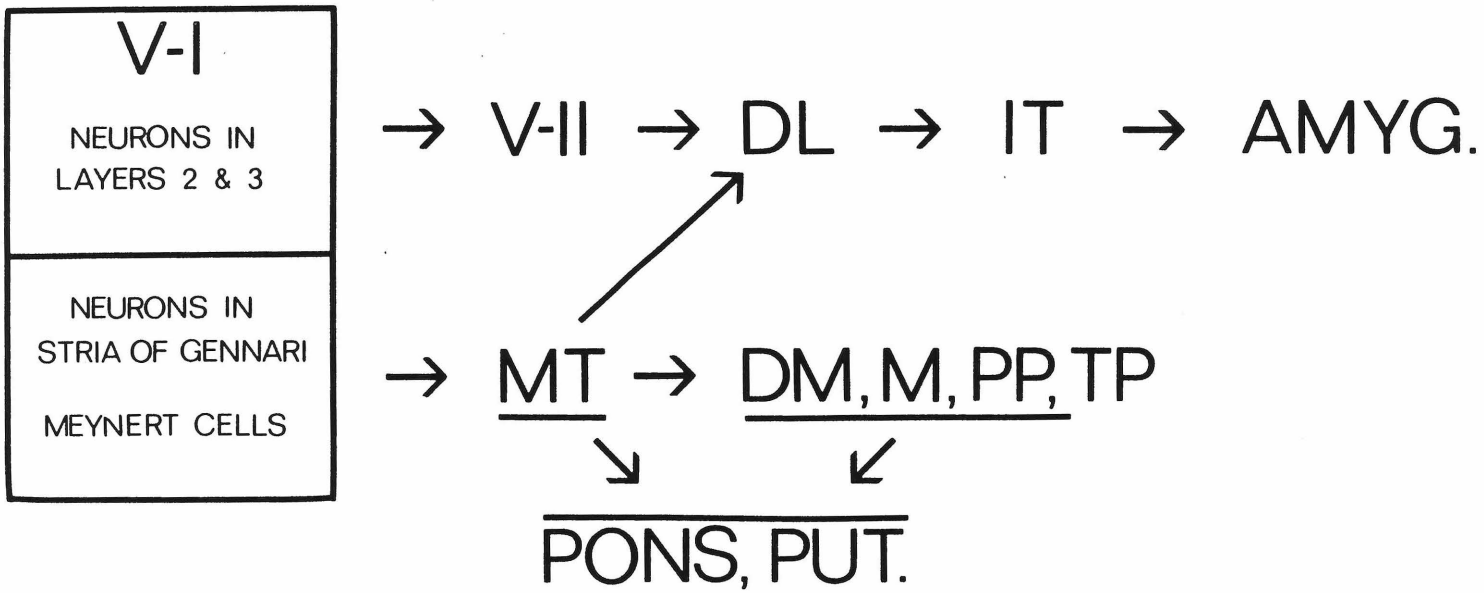
V-I
NEURONS IN LAYERS 2 & 3
NEURONS IN STRIA OF GENNARI
MEYNERT CELLS
→ V-II → DL → IT → AMYG.
→ MT → DM, M, PP, TP
PONS, PUT.

REFERENCES

1. Adrian, E. D. Double representation of the feet in the sensory cortex of the cat. J. Physiol., London **98**: 16P-18P, 1940.
2. Adrian, E. D. Afferent areas in the brains of ungulates. Brain **66**: 89-103, 1943.
3. Allman, J. M. and Kaas, J. H. A representation of the visual field in the caudal third of the middle temporal gyrus of the owl monkey (Aotus trivirgatus). Brain Res. **31**: 84-105, 1971.
4. Allman, J. M. and Kaas, J. H. Representation of the visual field in striate and adjoining cortex of the owl monkey (Aotus trivirgatus). Brain Res. **35**: 89-106, 1971.
5. Allman, J. M. and Kaas, J. H. The organization of the second visual area (VII) in the owl monkey: a second order transformation of the visual hemifield. Brain Res. **76**: 247-265, 1974.
6. Allman, J. M. and Kaas, J. H. A crescent-shaped cortical visual area surrounding the middle temporal area (MT) in the owl monkey (Aotus trivirgatus). Brain Res. **81**: 199-213, 1974.
7. Allman, J. M. and Kaas, J. H. The dorsomedial cortical visual area: a third tier area in the occipital lobe of the owl monkey (Aotus trivirgatus). Brain Res. **100**: 473-487, 1975.
8. Allman, J. M. and Kaas, J. H. Representation of the visual field on the medial wall of occipital-parietal cortex in the owl monkey. Science **191**: 572-575, 1976.
9. Clarke, E. and O'Malley, C. D. The Human Brain and Spinal Cord. Berkeley: University of California Press, 1968.
10. Fritsch, G. and Hitsig, E. Uber die electrische Erregbarkeit des Grosshirrs. Arch f. Anat., Physiol. and wissenschaftl, pp. 300-332, 1870.

11. Gattas, R. and Gross, C. G. A visuotopically organized area in the posterior superior temporal sulcus of the macaque. Ann. Meeting Assoc. Res. Vision Opthalmol., 1979, p. 184.

12. Hubel, D. H. and Wiesel, T. N. Receptive fields, binocular interaction, and functional architecture in the cat's visual cortex. J. Physiol., London **160**: 106-154, 1962.

13. Hubel, D. H. and Wiesel, T. N. Receptive fields and functional architecture in two non-striate visual areas (18 and 19) of the cat. J. Neurophysiol. **28**: 229-289, 1965.

14. Imig, T. J., Ruggero, M. A., Kitzes, L. M., Javel, E. and Brugge, J. F. Organization of auditory cortex in the owl monkey (Aotus trivirgatus). J. Comp. Neruol. **171**: 111-128, 1977.

15. Kaas, J. H., Nelson, R. J., Sur, M., Lin, C.-S. and Merzenich, M. M. Multiple representations of the body within "SI" of primates: A redefinition of "primary somatosensory cortex." Science **204**: 521-523, 1979.

16. Marshall, W. H., Talbot, S. A. and Ades, H. W. Cortical response of the anesthetized cat to gross photic and electrical efferent stimulation. J. Neurophysiol. **6**: 1-16, 1943.

17. Merzenich, M. M., Kaas, J. H., Sur, M. and Lin, C.-S. Double representation of the body surface within cytoarchitectonic areas 3b and 1 in SI in the owl monkey (Aotus trivirgatus). J. Comp. Neurol. **181**: 41-74, 1978.

18. McGuinness, E., Sivertsen, D. and Allman, J. M. Organization of the face representation in macaque motor cortex. J. Comp. Neurol. **193**: 591-608, 1980.

19. Merzenich, M. M. and Brugge, J. F. Representation of the cochlear partition on the superior temporal plane of the macaque monkey. Brain Res. **50**: 275-296, 1973.

20. Merzenich, M. M. and Kaas, J. H. Principles of organization of sensory-perceptual systems in mammals. Prog. Psychobiol. Phys. Psych. **9**: 1-41, 1980.

21. Newsome, W. T., Maunsell, J. H. R. and Van Essen, D. C. Areal boundaries and topographic organization of the ventral posterior area (VP) of the macaque monkey. Soc. Neurosci. Abstr. **6:** 579, 1980.

22. Palmer, L. A., Rosenquist, A. C. and Tusa, R. J. The retinotopic organization of lateral suprasylvian visual areas in the cat. J. Comp. Neurol. **177:** 237-256, 1978.

23. Polyak, S. The Vertebrate Visual System. Chicago: The University of Chicago Press, 1957.

24. Strick, P. L. and Preston, J. B. Multiple representation in primate motor cortex. Brain Res. **154:** 366-370, 1978.

25. Talbot, S. A. A lateral localization in cat's visual cortex. Fed. Proc. **1:** 84, 1942.

26. Tusa, R. J. and Palmer, L. A. The retinotopic organization of areas 20 and 21 in the cat. J. Comp. Neurol. **193:** 147-164, 1980.

27. Tusa, R. J., Palmer, L. A. and Rosenquist, A. C. The retinotopic organizaiton of the visual cortex in the cat. Soc. Neurosci. Abstr. **1:** 52, 1975.

28. Van Essen, D. C. Visual cortical areas. In: Ann. Rev. Neurosci., Vol. 2, edited by W. M. Cowan. Palo Alto: Annual Reviews, 1979, pp. 227-263.

29. Van Essen, D. C., Maunsell, J. H. R. and Bixby, J. L. The middle temporal area in the macaque: architecture, connections, functional properties and topographic organization. J. Comp. Neruol. **191:** 293-326, 1981.

30. Woolsey, C. N. and Fairman, D. Contralateral, ipsilateral and bilateral representation of cutaneous receptors in somatic areas I and II of the cerebral cortex of pig, sheep, and other mammals. Surgery **19:** 684-702, 1946.

31. Woolsey, C. N. and Walzl, E. M. Topical projection of the cochlea to the cerebral cortex of the monkey. Am. J. Med. Sci. **207:** 68 5-686, 1944.

Chapter 1

VISUAL RESPONSE PROPERTIES OF NEURONS IN OWL MONKEY EXTRASTRIATE CORTEX

INTRODUCTION

The discovery of a large number of extrastriate cortical visual areas has led to the hypothesis that each area performs its own set of functions in visual perception or visuomotor coordination (1-9, 35, 54, 58, 73, 75, 76, 78, 91). The representations are most numerous and the amount of cortex devoted to these representations most extensive in animals apparently specialized for complex uses of visual information, such as the cat (58, 75, 76) and various primates (1-9, 54, 78). Owl monkey visual cortex contains at least nine topographic representations of the visual field (3-8, 54) (see Fig. 1). We have studied functional localization in four extrastriate areas by making quantitative comparisons of the visual response properties of single neurons in the middle temporal (MT), dorsolateral (DL), dorsomedial (DM), and medial (M) areas. In this chapter the response properties of neurons in these areas to direction of movement, bar orientation, single spot and random dot stimuli are reported. Rather than attempt to classify neurons into categories, we have developed a series of indices computed for each cell for directionality tuning and other parameters through which we have assessed the similarities and differences among the populations of cells recorded from MT, DL, DM, and M. This work has been published (11, 55, 59).

METHODS

Seven owl monkeys were surgically prepared and used in weekly recording sessions. The preparatory surgery was performed under aseptic conditions and general anesthesia (Ketamine HCl, 25 mg/kg, IM, supplemented as needed). A stainless steel cylindrical chamber, 15 mm in diameter, with a threaded cap was positioned over an opening in the skull exposing extrastriate cortex and was cemented in place with Grip dental cement (L. D. Caulk Co., Milford, Delaware 19963). Thorough removal of the periosteum and application of primer and cement over a large portion of the skull insured a strong bond. The chamber could be positioned for microelectrode penetrations nearly perpendicular to the cortical surface, or for obliquely

Figure 1. The representations of the sensory domains in the cerebral cortex of the owl monkey. Above is a ventromedial view; below is a dorsolateral view. On the left is a perimeter chart of the visual field. The symbols in this chart are superimposed on the surface of the visual cortex. Pluses indicate upper quadrant representations; minuses, lower quadrants; dashed lines, borders of areas that correspond to the representations of the relatively peripheral parts of the visual field, but not the extreme periphery. The row of V's indicates the approximate border of visually responsive cortex. The dashed line broken by a question mark indicates an uncertain border. AI, first auditory area; AL, anterolateral auditory area; CC, corpus callosum; DI, dorsointermediate visual area; DL, dorsolateral crescent visual area; DM, dorsomedial visual area; IT, inferotemporal cortex; M, medial visual area; MT, middle temporal visual area; ON, optic nerve, OT, optic tectum; PL, posterolateral auditory area; PP, posterior parietal cortex; R, rostral auditory area; VA, ventral anterior visual area; VP, ventral posterior visual area; X, optic chiasm. The cortical visual areas were mapped by Allman and Kaas (3-8) and Newsome and Allman (54). The somatosensory areas were mapped by Merzenich et al. (51). The auditory areas were mapped by Imig et al. (38).

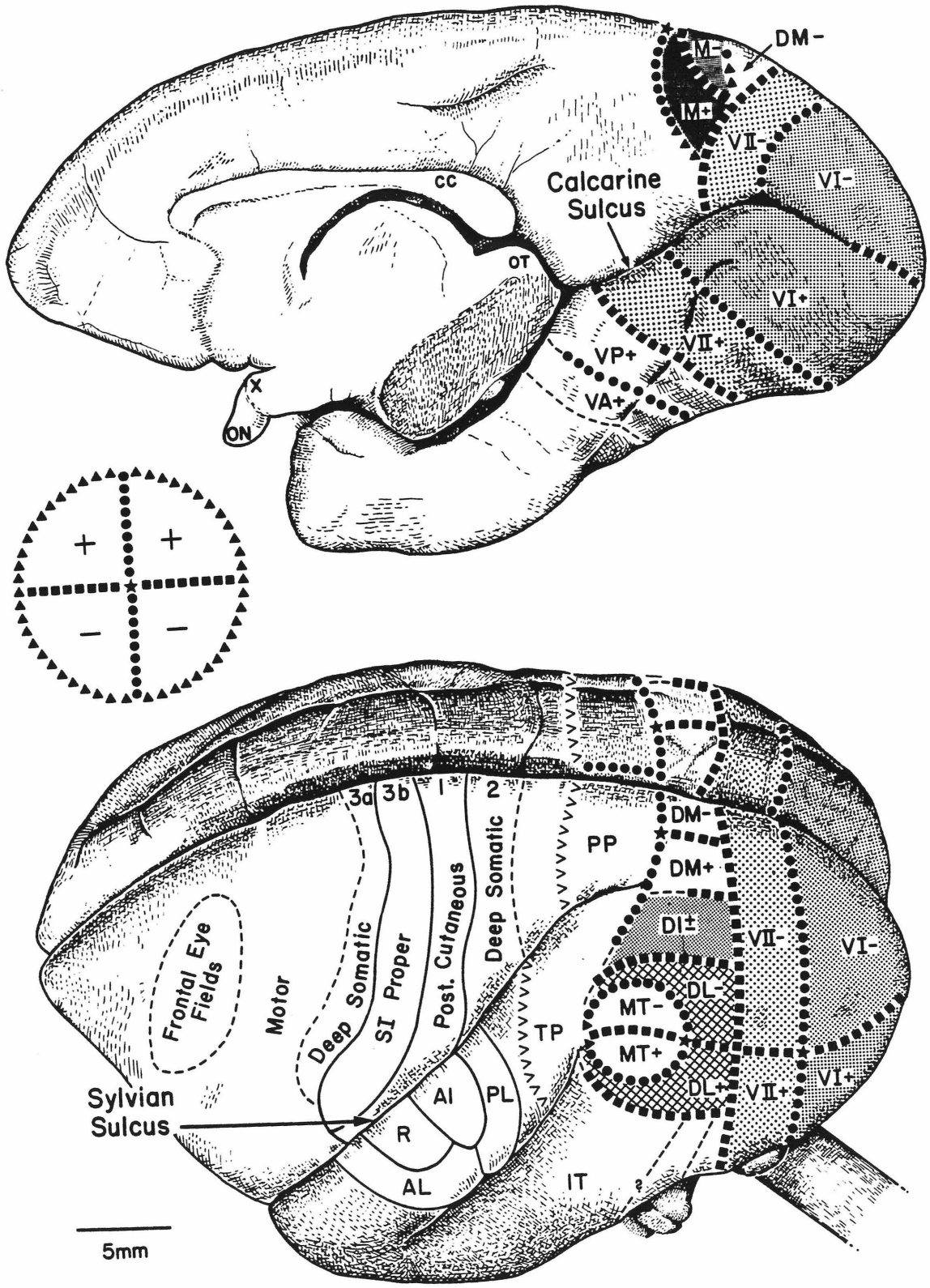
DM-
M-
M+
VII-
VI-
Calcarine Sulcus
cc
OT
VI+
VII+
VP+
VA+
X
ON
+
+
−
−
3a
3b
1
2
PP
DM-
DM+
DI±
VII-
VI-
DL-
MT-
MT+
DL+
VII+
VI+
TP
IT
Frontal Eye Fields
Motor
Deep Somatic
SI Proper
Post. Cutaneous
Deep Somatic
Sylvian Sulcus
AI
PL
R
AL
5mm

angled penetrations. After the chamber was in place, the exposed brain visible through the unopened dura mater was photographed for later reference. Within a few weeks a tissue growth covered the dura and obscured the cortex, and in some animals after several experiments it was necessary to remove this growth surgically so that microelectrodes could penetrate the cortex without being damaged.

At the outset of each experimental session a monkey was tranquilized with Vetame (Triflupromazine HCl, 5 mg/kg IM initial session, tapered to 2 mg/kg in later sessions). Very small doses of Ketalar (Ketamine HCl, 3-10 mg/kg/hr IM) were used to maintain sedation throughout the 12 to 14 hr session. The monkey's head was fixed in place with a circular clamp tightened around the recording chamber. This clamp was attached to a specially-designed monkey chair in which the animal was restrained in the normal owl monkey posture. Owl monkeys, like other New World monkeys, squat rather than sit as do Old World monkeys which possess ischial callosities, thus most commercially manufactured primate chairs are inappropriate for New World monkeys since they force the animal into an unnatural posture. The monkey was wrapped in a towel for warmth. The corneas, scleras, and eyelids were then topically anesthetized with a buffered solution of 0.5% Dibucaine HCl, and the pupils were dilated with Cyclogyl (Cyclopentolate 1%). After allowing the local anesthetic to take effect, the eyelids were retracted and held open with tape. Eye rings machined to fit the contour of the eye were cemented around the margins of the corneas with Histoacryl tissue adhesive (n-butyl-cyanoacrylate, B. Braun, Melsungen, West Germany), thus fixing the animal's gaze.

Contact lenses of +4 diopters power were used to protect the corneas from drying and bring the eyes into focus on a tangent screen 28.5 cm away. Images of the optic discs were projected onto the tangent screen with an ophthalmoscope (22), allowing the experimenters to check the focus and to bring the eyes into binocular alignment. Correct binocular alignment was achieved by adjusting ball joints to

which the eye ring stems were attached until the optic discs were projected at the same height on the screen and 40° apart. Superimposition of monocular receptive fields confirmed that 40° separation was the normal physiological position in all but one animal, for which 36-37° separation superimposed monocular fields. Care was taken not to torque the eyes or put pressure on the globe when positioning the eyes. Optic disc alignment was checked periodically during the session and at the end of the sessions before the eye rings were gently removed. The corneas remained in good condition throughout the course of these experiments. The owl monkey, like the owl, tends to move its eyes very little; the attachments of the extraocular muscles are placed far back on the globe relative to other monkeys and have a poor mechanical advantage. Thus this sytem provided good ocular stability.

The recording chamber was opened and cleaned with a mild solution of hydrogen peroxide (0.1%), then filled with warm mineral oil and sealed by the attachment of the microelectrode positioning device. This device could be rotated on the chamber, and the microelectrode advance mechanism was mounted on a calibrated slide, thus establishing a polar coordinate system. Glass insulated platinum-iridium microelectrodes were used to penetrate the dura and record the activity of single neurons (85). All materials coming into contact with the interior of the recording chamber were sterile.

Initial microelectrode placements in an experimental animal were guided by the need to construct a map of the exposed extrastriate cortex based on the visual field positions of single unit and background responses. Progressions of receptive fields from the upper visual quadrant to the lower quadrant and reversals of progressions at the vertical and horizontal meridians were used to locate the extrastriate areas and their boundaries by comparison with the known organization of owl monkey visual cortex shown in Fig. 1. Usually, two or three extrastriate areas were studied in an animal. Most units could be unambiguously assigned to a particular area. However,

some units (126/480) were recorded at area boundaries, or near uncertain area boundaries, and these were excluded from the data analyses reported here. Assignment of units to extrastriate areas was based solely on receptive field progressions and/or histological reconstructions, and all units which could be classified were included in the data analyses.

The visual responses of extrastriate units were studied both qualitatively and quantitatively. A unit was considered to be isolated well enough for study when its impulse could be made to trigger an oscilloscope sweep reliably, as determined by stored waveform superimposition. When a unit was isolated, a suitable stimulus was found and the receptive field was plotted with hand-controlled stimuli while listening to the unit's activity over an audio monitor. An estimate was made of the unit's preferred stimulus parameter values, then quantitative study was begun using computer-controlled stimuli. After quantitative study, a final qualitative assessment was made to reconfirm the unit's characteristics.

Quantitative evaluation of unit properties was done by computer routines developed for a Data General Nova 2 computer primarily by Francis Miezin. These programs controlled a rear projection optic stimulator equipped with galvanometer mirrors, stepping motors, and an electric shutter. The computer operated these peripheral devices to control stimulus orientation, direction of movement, velocity, shape, and size. Normally, one of these parameters was varied in a pseudorandom sequence of 8 to 12 values, and the sequence was presented 5 times. Repeated pseudorandomized presentations were necessary to avoid possible habituation effects (35), and to minimize the effects of trial-to-trial variability in extrastriate unit responses. The interstimulus interval was 6 s, with the 3 s immediately preceding the stimulus presentation used for estimating spontaneous activity. Parameters not being studied were held at their estimated best value. When a unit responded well to a light or dark bar stimulus, the effect of varying the orientation and direction of a moving

bar was studied first. The responses were displayed as they occurred on an oscilloscope as peristimulus-time histograms. As soon as the 5 runs of the stimulus sequence were completed, the orientation tuning of the unit was displayed on a polar plot. The optimal orientation was then used when studying other parameters with elongated stimuli. Responses were studied to different velocities, directions of spot movement, bar lengths, widths, spot sizes, and random dot stimuli. The random dot stimuli consisted of a fixed 40° area centered on the receptive field and in which randomly spaced small spots (density = 10%, 0.5° or 1.3° diam. spots) moved in the same direction at a uniform velocity. In addition to the immediate display of results, the time of occurrence of each impulse and the stimulus parameter values were stored on magnetic disc for later analysis.

A second set of programs was used for off-line data analysis. A neuron's spontaneous firing rate (spikes/s) in the 3-s interval before stimulus presentation was subtracted from its firing rate during the stimulus presentation to yield the net response rate for a single sweep. The stimulus sweep was adjusted to extend slightly beyond a unit's receptive field boundaries. The average net response rate over the 5 identical sweeps in the repeated pseudorandom sequence was used in subsequent calculations to compare responses at different parameter values, and, after normalizing the data, to compute various indices of stimulus selectivity.

The programs then classified these indices and other unit data into groups by extrastriate areas, and statistical tests (F-tests, t-tests, linear regression, correlations) were performed on the grouped data to determine whether data were significantly different across areas, and which indices were correlated within an area or across all areas.

The physiologically derived maps of extrastriate cortex were confirmed by histology done on three animals. Small electrolytic lesions (10 μA for 10 s) were placed at one to three locations along selected penetrations. At the termination of

the final unit recording session the monkey was deeply anesthetized with a lethal dose of sodium pentobarbitol and then perfused with 0.9% saline followed by 3.7% formaldehyde in 0.9% saline. The head was mounted in the experimental position, and marking pins were placed at designated coordinates to aid electrode track reconstruction. The brain was removed from the skull, photographed, and placed in 30% sucrose in formol-saline. Alternate 40-μ frozen sections were stained with cresyl violet for cell bodies and hematoxylin for myelin. The heavy myelination of MT, visible even in unstained sections, was the most readily identified myeloarchitectonic feature (3). Histological reconstruction confirmed the area designations determined by receptive field progressions.

RESULTS

Neurons in all four areas shared certain response properties. An appropriately sized bar of a particular orientation, direction, and velocity of movement through a neuron's receptive field was nearly always an effective stimulus, although a few exceptions will be noted below. Hand-mapped receptive fields were homogeneously excitatory. Computer-controlled raster maps of 21 cells confirmed the homogeneity of the receptive fields, showing no strong inhibitory regions. In DM, M, and MT, responses for most cells summated for stimuli up to the length of the receptive fields and were unaffected by further increases in length (60). In DL, the preferred stimulus length for 70% of the cells was much smaller than the length of the receptive field. The results are presented below as distributions of response properties rather than as arbitrary classes of cells. Most distributions were unimodal, and thus did not provide the natural bases for class divisions. Exceptions included the flashed bar and random dot response distributions; some cells in certain areas were unresponsive to these types of stimuli.

Figure 2. Calculation of the direction and tuning indices for representative neurons from MT (top) and a neuron from DM (bottom). Directions of motion at which stimuli were presented are plotted horizontally. The neuronal response for stimuli moving in each direction as a percentage of the optimal response is plotted vertically. The illustrated response in each direction is the arithmetic mean of the individual responses to the five stimulus presentations. Formulas for computation of direction and tuning indices are given at the bottom. The shaded area for each response curve is the area under the curve computer for calculation of the tuning index. The direction index may be greater than one if spontaneous firing is inhibited by stimuli directed opposite to the optimum direction, as is the case for the upper neuron. In the calculation of the tuning index, if the spontaneous firing rate is inhibited in some of the directions within $\pm$ 90° of the optimum, the area under the curve is the algebraic sum of the areas above and below the zero response level (areas of inhibition being negative). This situation obtains for the upper neuron.

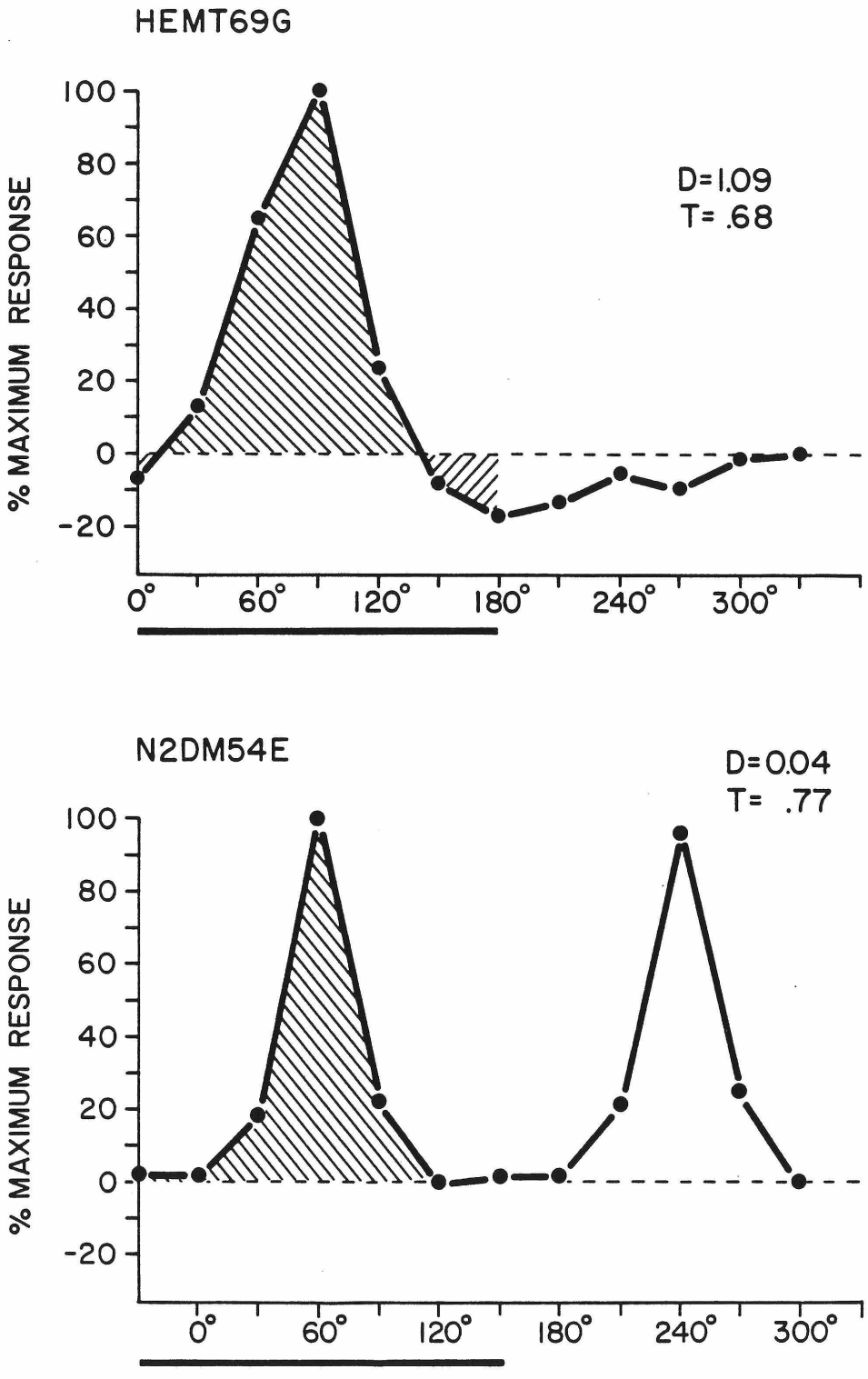
HEMT69G
% MAXIMUM RESPONSE
100
80
60
40
20
0
-20
D=1.09
T= .68
0°
60°
120°
180°
240°
300°
N2DM54E
% MAXIMUM RESPONSE
D=0.04
T= .77
'D' INDEX = 1 - OPP./BEST
'T' INDEX = 1 - (AREA UNDER CURVE)

Responses to moving bars

The most important factors affecting the responses of the majority of extrastriate neurons studied were the direction and orientation of a moving stimulus. These were first assessed for each neuron with a bar stimulus oriented perpendicular to its direction of movement, which was swept through the receptive field in a pseudorandomly ordered sequence of twelve directions separated by 30° intervals that was repeated five times. This bar direction/orientation series was run on a total of 480 cells, 56 in M, 89 in DM, 80 in DL, 129 in MT, and 126 which could not be assigned to a particular area.

A neuron's spontaneous firing rate was subtracted from the mean firing rate during the stimulus presentation to obtain response rates which were averaged for the five sweeps in a particular direction. Responses were normalized to a percentage of the maximum response and displayed as in Fig. 2, which shows responses as a function of bar stimulus direction for a cell in MT (top) and a cell in DM (bottom). Two response measures were calculated from these data, a direction index, which compared the response in the best direction of movement with the response in the direction 180° opposite, and a tuning index, which compared the response in the best direction with those to directions within $\pm$ 90°. The formula used for calculating the direction index was one minus the ratio of the response in the 180° opposite direction to the response in the best direction. Thus for the cell illustrated at the bottom of Fig. 2, the ratio of opposite response to best response was almost one, and the direction index almost zero. For the cell illustrated at the top of Fig. 2, the direction index was approximately one, exceeding this value because spontaneous firing was inhibited in the opposite direction. Previously described direction selective cells (12) would have high direction indices.

The distributions of direction indices for cells in the four extrastriate areas studied are shown in Fig. 3. Cells in M and DM had consistently low direction indices,

Figure 3. Distribution of direction indices for DM, DL, MT, and M. MT neurons are strongly grouped near a direction index of 1.0, which differs markedly from the distributions present in DM, DL, and M. An analysis of variance was performed on these data (62). The value of S (Scheffe's multiple comparisons) for MT versus DM was 10.89; MT versus M was 9.37; MT versus DL was 3.5; p is very much smaller than 0.01 for the MT-DM and MT-M differences and less than 0.02 for the MT-DL differences.

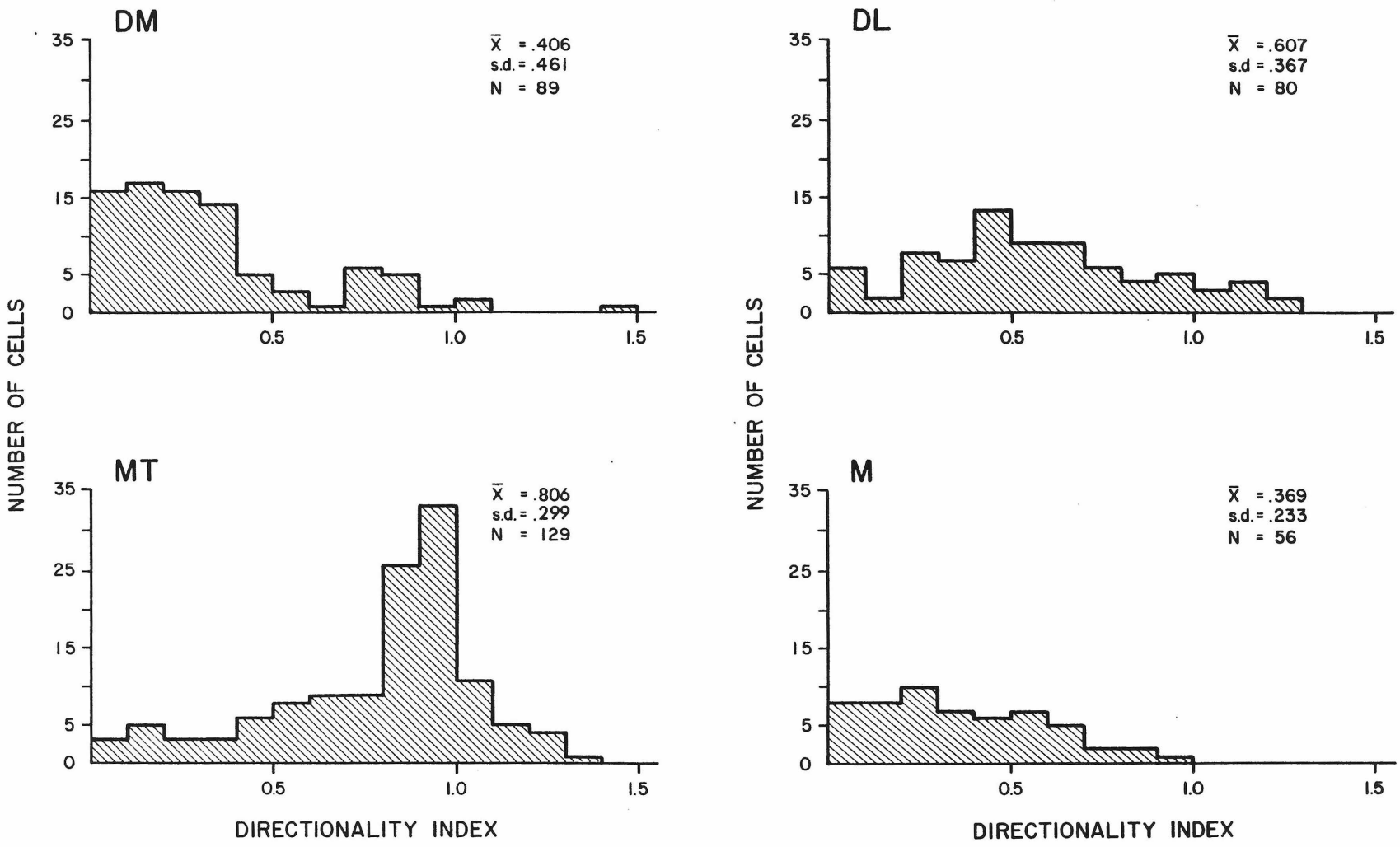
DM
$\bar{X}$ = .406
s.d. = .461
N = 89
DL
$\bar{X}$ = .607
s.d = .367
N = 80
MT
$\bar{X}$ = .806
s.d. = .299
N = 129
M
$\bar{X}$ = .369
s.d. = .233
N = 56
NUMBER OF CELLS
NUMBER OF CELLS
0
5
15
25
35
0.5
1.0
1.5
DIRECTIONALITY INDEX
DIRECTIONALITY INDEX

while MT cells usually had high direction indices. The direction indices of DL cells varied widely.

The statistical test used was a one-way analysis of variance with comparisons being made between areas using Scheffe's multiple comparisons (62, see Fig. 3 for s-values). We assumed that recordings made in the same area of different animals were from the same population.

The tuning index measured a cell's selectivity for the best direction of movement as compared with other directions within 90°. The normalized area under the tuning curve out to 90° on either side of the best direction (the shaded area in Fig. 2) was subtracted from one to yield the tuning index. The area measured was restricted to $\pm$ 90° so that the tuning for bidirectional and directionally selective cells could be measured on the same scale. The tuning index is close to one for sharply tuned cells and close to zero for very broadly tuned cells. When spontaneous firing was inhibited in some of the relevant directions the area under the curve was taken as the difference between the areas above and below the spontaneous level. This inhibition was uncommon and, when present, was usually weak. The distributions of tuning indices for M, DM, DL, and MT are illustrated in the histograms of Fig. 4. Although the differences are not as striking as for the direction index, an analysis of variance showed that DM cells were significantly more sharply tuned than M ($p < 0.02$), DL ($p < 0.01$), and MT ($p < 0.02$) cells. The average response magnitude and signal-to-noise ratios are shown in Table 1.

Two-dimensional plots of the cells' tuning and directionality indices are shown for the four areas in Fig. 5. The bulk of the data for an area falls in a single region of its graph. The different location of this region in each graph is an indication of the differences among the areas. There is no evidence in the form of multiple clusters on a graph, which would suggest multiple classes of cells within an area. Figure 5 also shows the small but significant correlation between directionality and tuning in DL ($r=0.47$), DM ($r=0.29$), and MT ($r=0.34$).

Figure 4. Distribution of tuning indices for DM, DL, MT, and M. Cells in DM tend to be more sharply tuned than cells in the other areas. An analysis of variance was performed on these data (62). The value of S (Scheffe's multiple comparisons) for DM versus DL was 7.66; DM versus MT was 3.5; DM versus M was 3.41; p is very much smaller than 0.01 for the DM-DL difference and less than 0.02 for the DM-MT and DM-M differences.

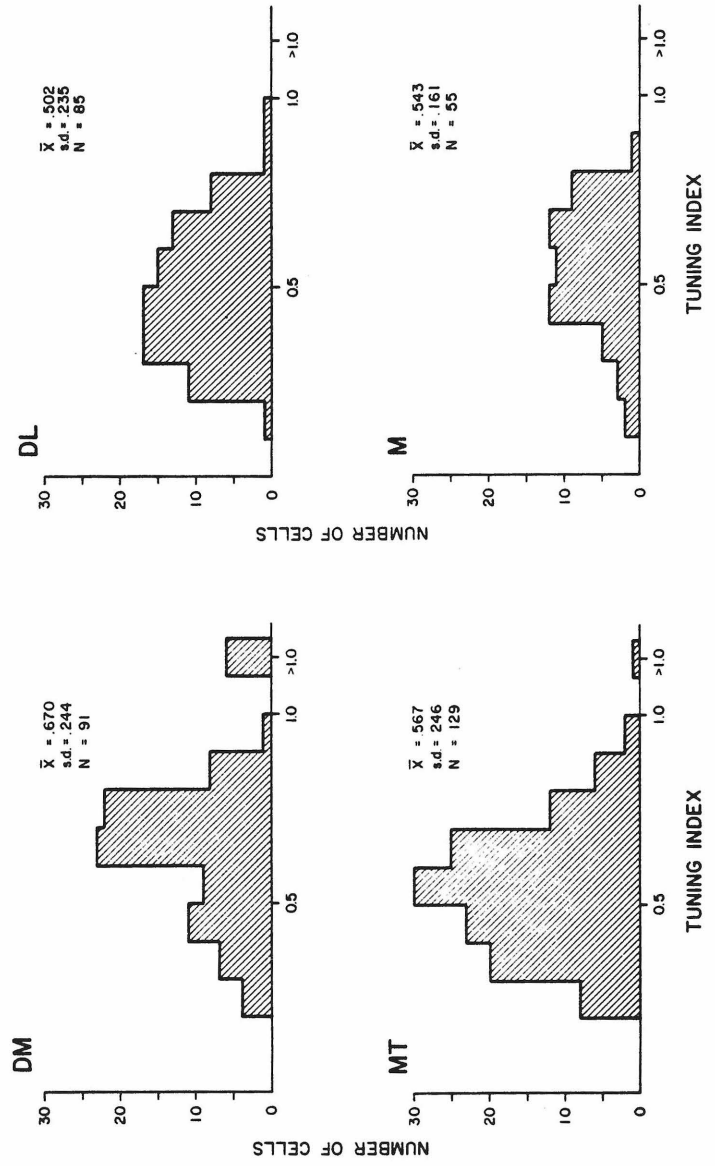
DL
$\bar{X}$ = .502
s.d. = .235
N = 85
M
$\bar{X}$ = .543
s.d. = .161
N = 55
DM
$\bar{X}$ = .670
s.d. = .244
N = 91
MT
$\bar{X}$ = .567
s.d. = .246
N = 129
NUMBER OF CELLS
TUNING INDEX
0
10
20
30
0.5
1.0
>1.0

Figure 5. Two-dimensional plots of tuning and directionality indices for cells in DL, DM, M, and MT. The size of a dot represents the percentage of cells that have appropriate values for the two indices. Each area has a high concentration of cells in a single region of its graph; for example, DM cells generally have low direction indices and high tuning indices.

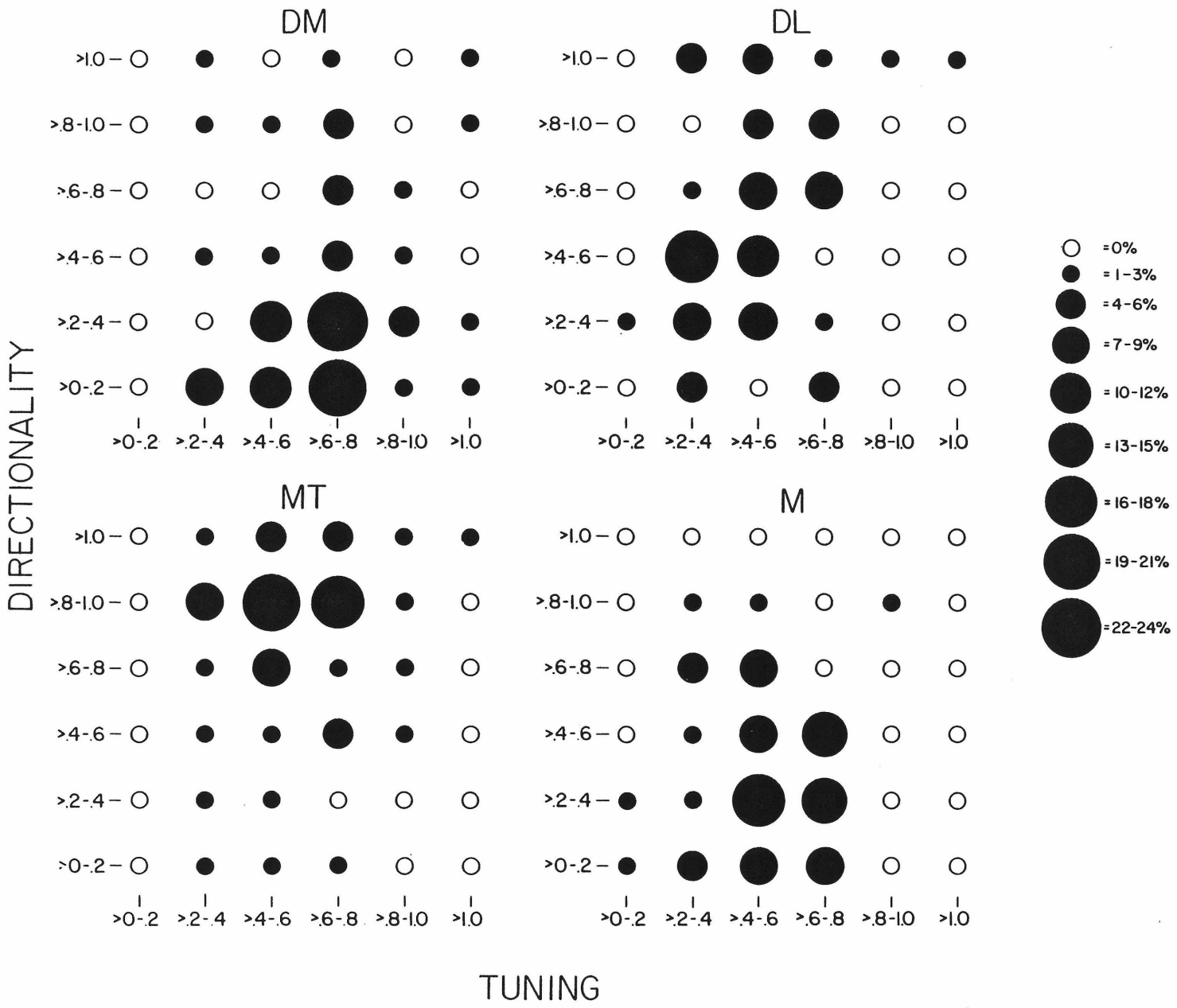
DM
DL
MT
M
DIRECTIONALITY
TUNING
>1.0
>.8-1.0
>.6-.8
>.4-.6
>.2-.4
>0-.2
>0-.2
>.2-.4
>.4-.6
>.6-.8
>.8-1.0
>1.0
=0%
=1-3%
=4-6%
=7-9%
=10-12%
=13-15%
=16-18%
=19-21%
=22-24%

Responses to moving spots

Direction series were also run with moving spot stimuli to test direction sensitivity in the absence of an oriented stimulus (71). Many neurons in M and DM, most notably DM, responded quite poorly to small spot stimuli. Fifteen of 23 DM cells tested with spots of various diameters showed summation up to or beyond 15° diameter, so discs up to 13° diameter were used to obtain good responses, although in every case the test spot was smaller than the tested neuron's mapped receptive field. Smaller spots evoked good responses from many DL cells (60) and were used to minimize the possibility that the disc stimulus acted as an approximate edge oriented orthogonal to its direction of movement. In every extrastriate area studied, the tuning indices for directions of spot movement (M, $\bar{X} = 0.462$; DM, $\bar{X} = 0.449$; DL, $\bar{X} = 0.390$; MT, $\bar{X} = 0.45$) were significantly lower than the tuning indices for direction of bar movement (DM, DL, MT, $p < 0.005$; M, $p < 0.025$). Ninety-four of 120 cells were more sharply tuned to bars than to spots. The distribution of direction indices for bar stimuli was not significantly different from the distribution of direction indices for spot stimuli in any area.

Responses to flashed bars

The presentation of pseudorandomly ordered orientations of flashed bar stimuli was used to test orientation sensitivity in the absence of movement. Responses to flashed bar stimuli were obtained from all areas, though some cells were unresponsive (9/106 cells), and others responded only weakly. A cell generally responded transiently to the onset of a bar flashed at the optimal orientation (as determined with a moving bar stimulus), with a minority of cells (29/106) showing a clear off-response. Occasionally (2/106) a cell was encountered which gave only an "off" response. Only the responses to stimulus onset were used in the data analysis for this study. The tuning indices to stationary bar stimuli were high, as shown in the histograms of Fig. 6a; in each area, the average tuning index for stationary flashed

Figure 6. A. The distributions of tuning indices to oriented stationary flashed bar stimuli. The tuning indices were significantly higher in DM than in DL and DM, and higher in MT than DL ($p < 0.05$).

B. Distributions of the differences between each cell's flashed bar and moving bar tuning indices for each area.

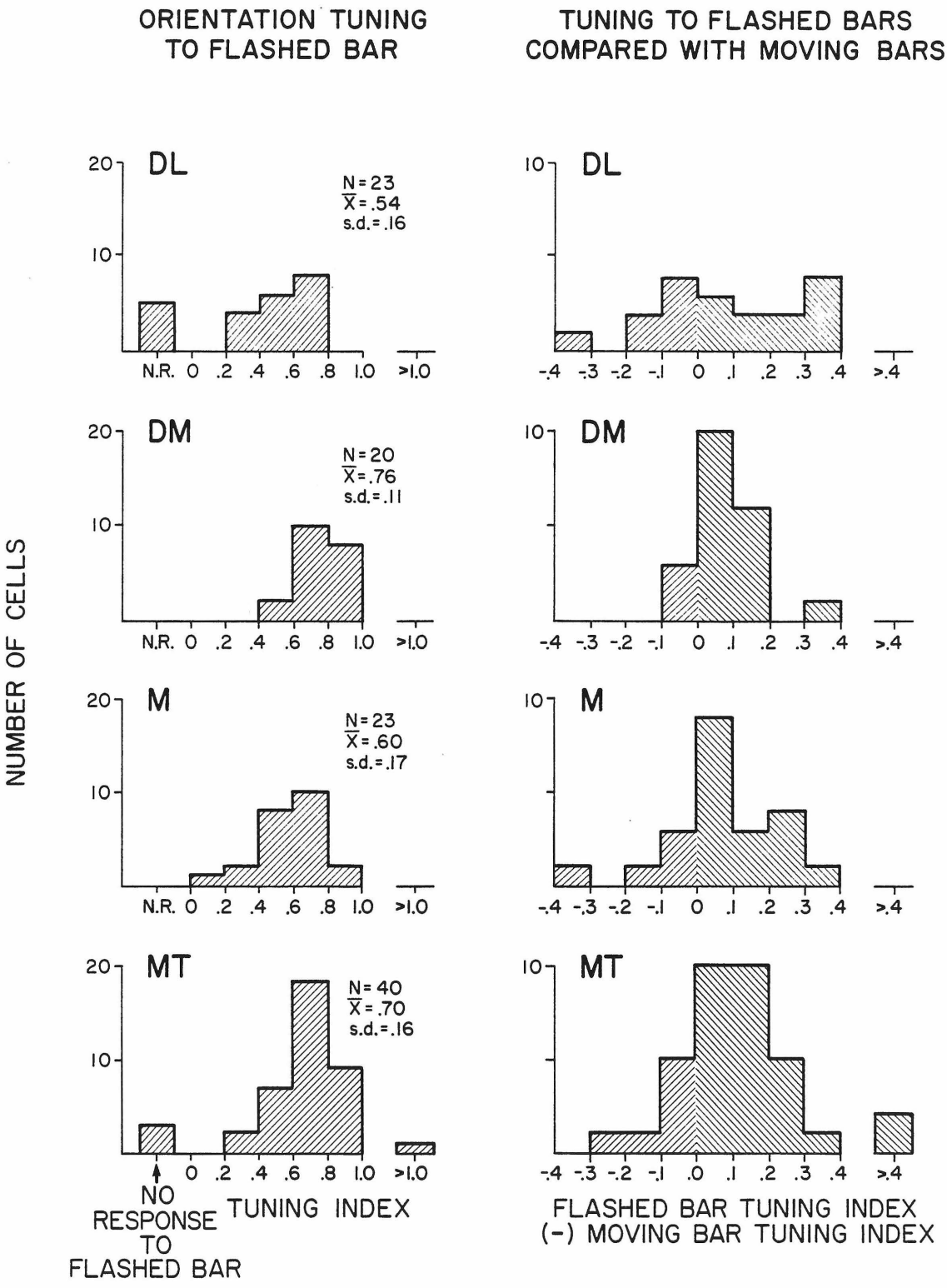
ORIENTATION TUNING
TO FLASHED BAR
TUNING TO FLASHED BARS
COMPARED WITH MOVING BARS
NUMBER OF CELLS
DL
N=23
X̄=.54
s.d.=.16
DM
N=20
X̄=.76
s.d.=.11
M
N=23
X̄=.60
s.d.=.17
MT
N=40
X̄=.70
s.d.=.16
20
10
N.R. 0 .2 .4 .6 .8 1.0 >1.0
-.4 -.3 -.2 -.1 0 .1 .2 .3 .4 >.4
NO RESPONSE TO FLASHED BAR
TUNING INDEX
FLASHED BAR TUNING INDEX
(-) MOVING BAR TUNING INDEX

bars was higher than for moving bars. Figure 6b shows the distribution of differences between a cell's flashed and moving bar indices for each area. Orientation tuning was tested with flashed bars centered in two or more different regions of the receptive field of three neurons; the optimal orientation was independent of the position of the stimulus in the field. There was no significant difference between the flashed bar tuning of cells with high direction indices and cells with low direction indices.

Responses to moving random dot patterns

For some cells, most frequently encountered in MT, the most effective stimulus among those tested was not a bar or a spot, but an array of randomly spaced small dots moving in the same direction at a uniform velocity within a stationary window 40° in diameter. Outside the window, the field was uniformly illuminated. Figure 7 shows for cells in the four areas, the comparison between the mean response to an optimally oriented bar stimulus moving in its best direction and the mean response to a random dot array moving in its best direction. Sixteen of 31 MT cells tested with both random dot arrays and the quantitatively determined optimal bar stimulus orientation and direction responded better to the array. The median signal-to-noise ratio for random dot responses in MT was much higher than for the other areas and also was the highest for any class of stimuli tested in any area (see Table I). Cells in M were also often quite responsive to the dot arrays (optimal stimulus for six of 21 cells tested), while DM (8/13) and DL (8/21) cells were frequently unresponsive.

Responses to stimulus velocity

The large majority of neurons in all four extrastriate areas fired best at a velocity in the 10-100°/s range. We chose the mean response rate during the stimulus sweep as our velocity response measure; this represents a compromise between total spikes per sweep and peak rate measures, which emphasize low and high velocity responses, respectively (61). Typical examples of velocity tuning curves for a cell from DL and one from M are shown in Fig. 8. There was no uniform shape of velocity

TABLE 1

Average best response in spikes per second

	Moving Bar			Single Spot			Flashed Bar			Random Dots		
Area	N	$\bar{x}$	s.d.	N	$\bar{x}$	s.d.	N	$\bar{x}$	s.d.	N	$\bar{x}$	s.d.
DL	80	13.14	11.56	51	13.08	12.93	23	4.94	4.48	21	2.54	3.74
DM	89	14.12	15.57	25	8.85	11.64	20	8.16	7.12	13	3.89	4.63
M	56	20.65	17.18	32	21.08	23.73	22	12.03	10.09	21	21.74	19.46
MT	129	14.40	14.63	51	14.74	17.48	37	9.35	12.52	31	15.33	14.89

Median signal-to-noise ratio

Area	N	S/N	N	S/N	N	S/N	N	S/N
DL	80	14.48	51	13.37	N	4.00	21	2.54
DM	89	13.13	25	8.82	20	15.31	13	2.50
M	56	13.42	32	7.50	22	7.80	21	10.30
MT	129	24.73	51	24.00	37	10.98	31	37.50

(Continues)

	Best response to particular stimulus type								
	Best response to moving bar								
	Single Spot			Flashed Bar			Random Dots		
Area	N	$\bar{x}$	s.d.	N	$\bar{x}$	s.d.	N	$\bar{x}$	s.d.
DL	39	.97	.64	23	.75	.63	20	.40	.61
DM	25	.74	.59	20	.85	.66	13	.25	.42
M	24	.78	.56	21	.62	.43	19	.83	.51
MT	43	.93	.63	34	.66	.65	31	1.13	.59

Legend for Table 1

The signal-to-noise ratio was calculated for each cell by dividing its mean discharge rate for the optimal direction of movement or orientation by its average spontaneous activity. Median signal-to-noise ratios were used because cells with little or no spontaneous activity have very large signal-to-noise ratios, and would tend to skew the mean ratios to a level that does not reflect their actual distributions.

Figure 7. Comparison between the response to an optimally oriented bar moving in its optimal direction at optimal velocity with the response to a moving array of random dots for DM, DL, MT, and M. The response to the moving array is expressed as a percentage of the response to the bar.

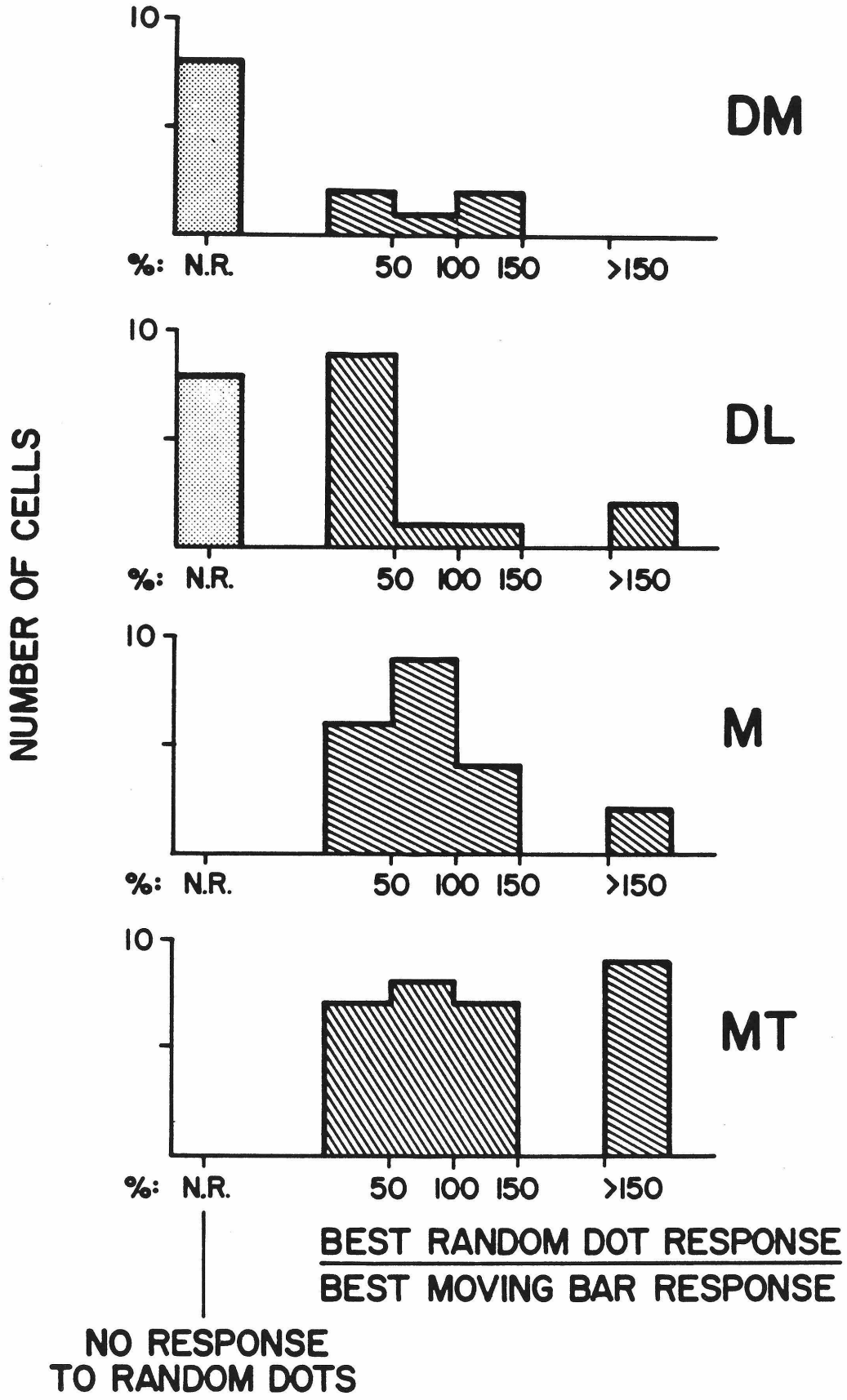
NUMBER OF CELLS
10
DM
%: N.R. 50 100 150 >150
10
DL
%: N.R. 50 100 150 >150
10
M
%: N.R. 50 100 150 >150
10
MT
%: N.R. 50 100 150 >150
BEST RANDOM DOT RESPONSE
BEST MOVING BAR RESPONSE
NO RESPONSE
TO RANDOM DOTS

tuning curves; the majority of cells were broadly tuned, but sharply tuned cells, low pass responses, and high pass responses were occasionally encountered. Overall, as displayed in Fig. 9, DL and MT contained a larger share of neurons which responded optimally at lower velocities around 10°/s, although both these areas contained some neurons which responded best at quite high velocities. Fourteen of 69 MT cells tested gave their optimal response at a velocity over 100°/s. Some MT cells fired well to a 500°/s stimulus, the highest velocity tested. DM neurons preferred intermediate velocities, and M cells preferred higher velocities. There was no correlation between the optimal velocity and the sharpness of tuning about that velocity ($r = 0.12$). Two neurons were encountered which did not respond to any smoothly moving stimulus but were excited by erratic small displacements produced under hand stimulus control.

Vertical organization of MT

Long penetrations nearly perpendicular to the cortical surface were made in MT to investigate systematic differences between superficial and deep cells in their orientation, direction, and random array stimulus responses. The responses of a series of single neurons in a penetration in MT, which histological reconstruction showed to be perpendicular to the cortical surface and nearly parallel to the radial fibers, is illustrated in Fig. 10. The graphs on the right show the average response of each neuron to six different orientations each presented 10 times in pseudorandom order. The dotted line indicates the level of spontaneeous activity for each neuron. Neuron A was broadly tuned; B through K all strongly preferred horizontally oriented bars; L was strongly inhibited by horizontal bars and thus was the negative complement of the other cells in the penetration. These data, together with other data we have obtained, suggest the presence of vertical columns of orientation selective neurons in MT such as have been described for the primary visual area (V-I) (37). The graphs on the left show the average response of each neuron to moving bar stimuli crossing the receptive field in 12 different directions. In each case the bar

Figure 8. Example of a cell in DL preferring a slow velocity (top) and a cell in M preferring a relatively high velocity (bottom). The response measure was mean spikes/second during the stimulus sweep.

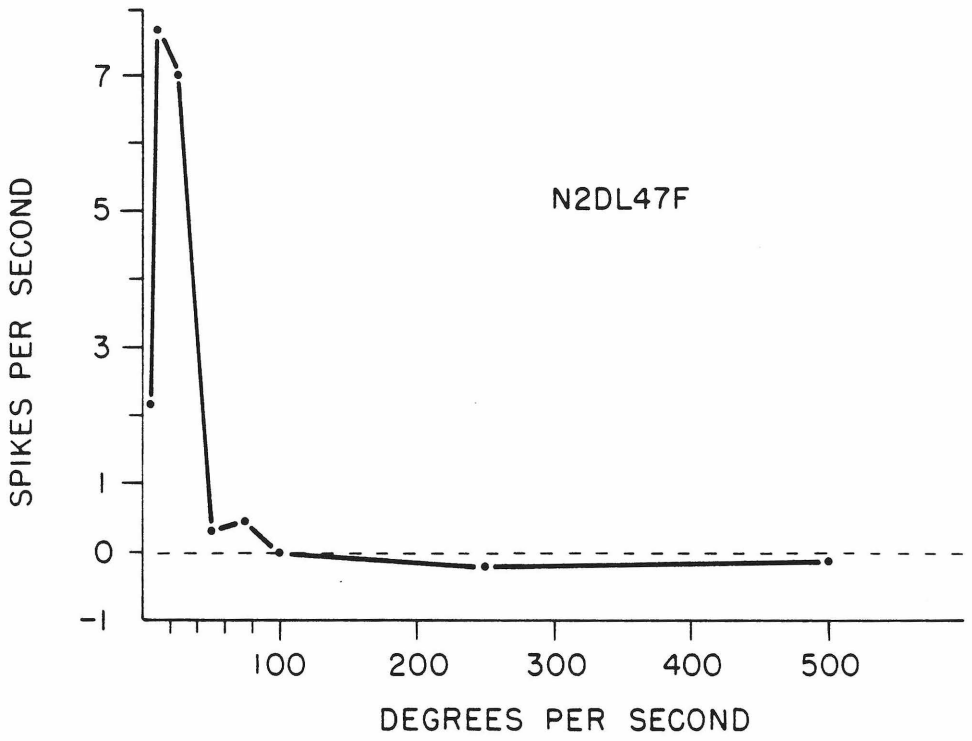
N2DL47F
SPIKES PER SECOND
7
5
3
1
0
-1
100
200
300
400
500
DEGREES PER SECOND

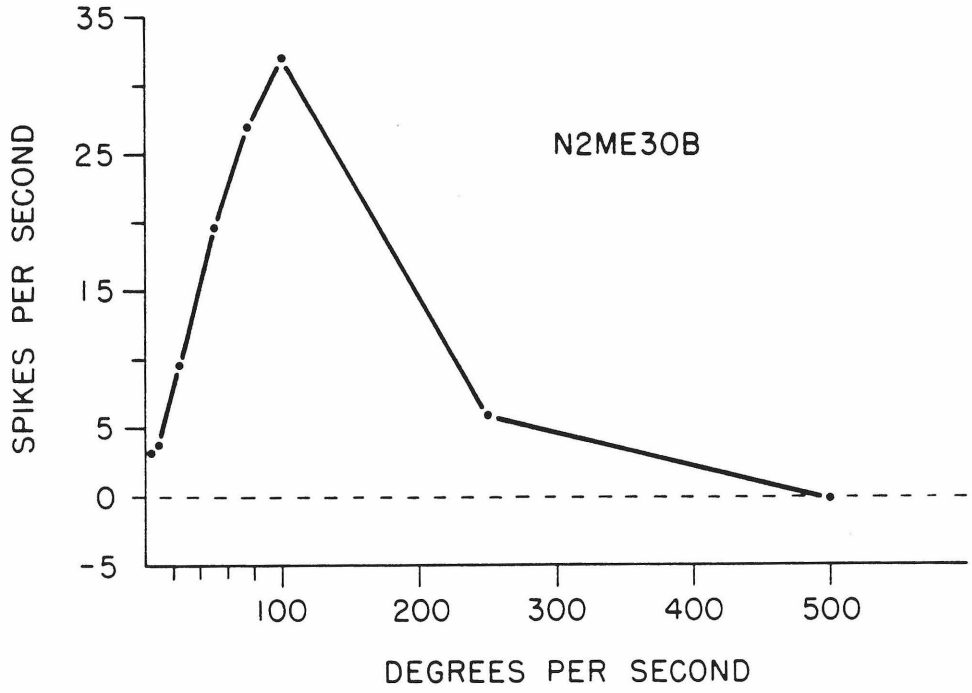
N2ME30B
SPIKES PER SECOND
35
25
15
5
0
-5
100
200
300
400
500
DEGREES PER SECOND

VELOCITY

Figure 9. Distributions of preferred velocities for neurons in DM, DL, MT, and M.

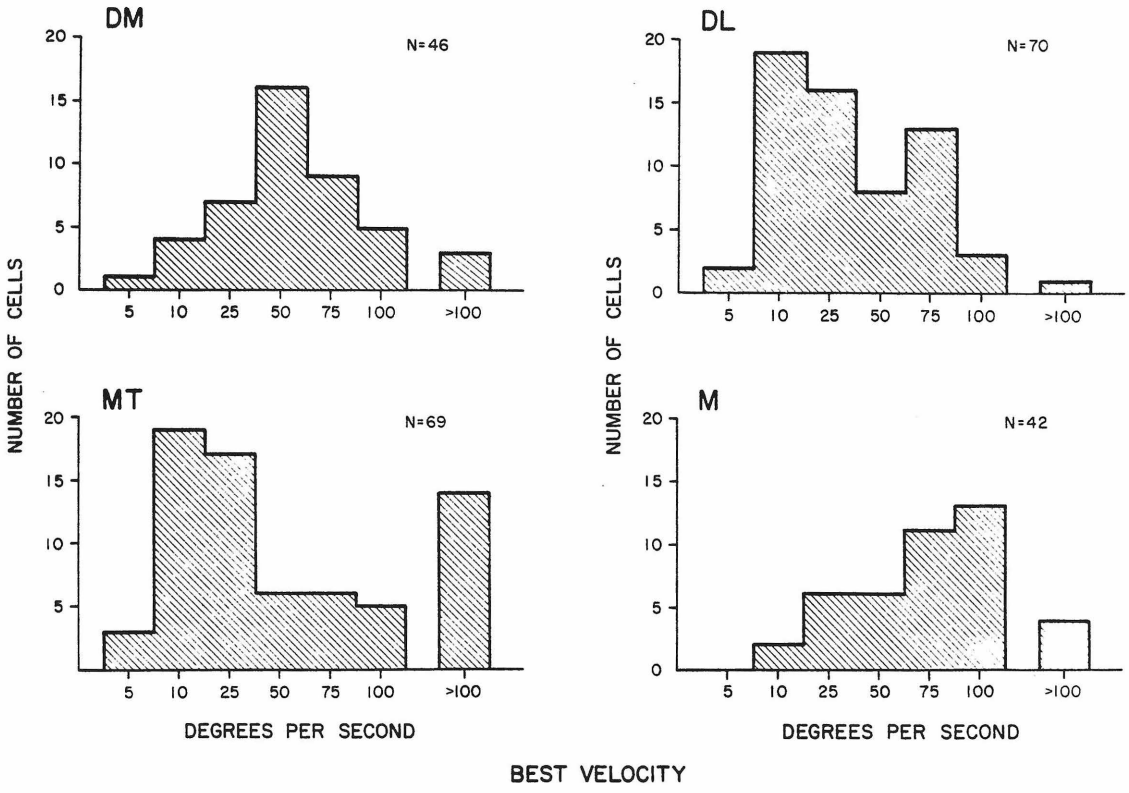
DM
N=46
DL
N=70
MT
N=69
M
N=42
NUMBER OF CELLS
NUMBER OF CELLS
0
5
10
15
20
5
10
25
50
75
100
>100
DEGREES PER SECOND
DEGREES PER SECOND
BEST VELOCITY

Figure 10. Direction and orientation selectivity for a series of neurons recorded in a single penetration nearly perpendicular to the surface of MT. A pair of graphs is illustrated for each unit (HEMT69 A through L). The depth beneath the surface at which each cell was recorded is given beneath each identifying number. An electrolytic lesion was made at the bottom of the microelectrode track. Histological reconstruction indicated that the penetration was perpendicular to the surface of MT and nearly parallel to the radial fibers. Cells A through J were located in layers II and III; cells K and L were located in layer IV. The graphs on the left illustrate the average response of each cell to 5 presentations of a 20° x 1° light bar at 12 different angles. HEMT69 A through F preferred 270°; HEMT69 G through K preferred 90°. The graphs on the right illustrate the average response of the cells to 10 presentations of a flashed bar at the orientations shown. All of the cells except the last preferred the horizontal orientation; the last was inhibited by horizontal bars. The direction of movement was 90° to the bar orientation, thus the preferred directions of 270° (down) and 90° (up) are consistent with the preferred horizontal orientation. The receptive field centers were located an average of 16.6° below the horizontal meridian with a standard deviation of 0.9°, and an average of 6.7° temporal to the vertical meridian with a standard deviation of 3.3°.

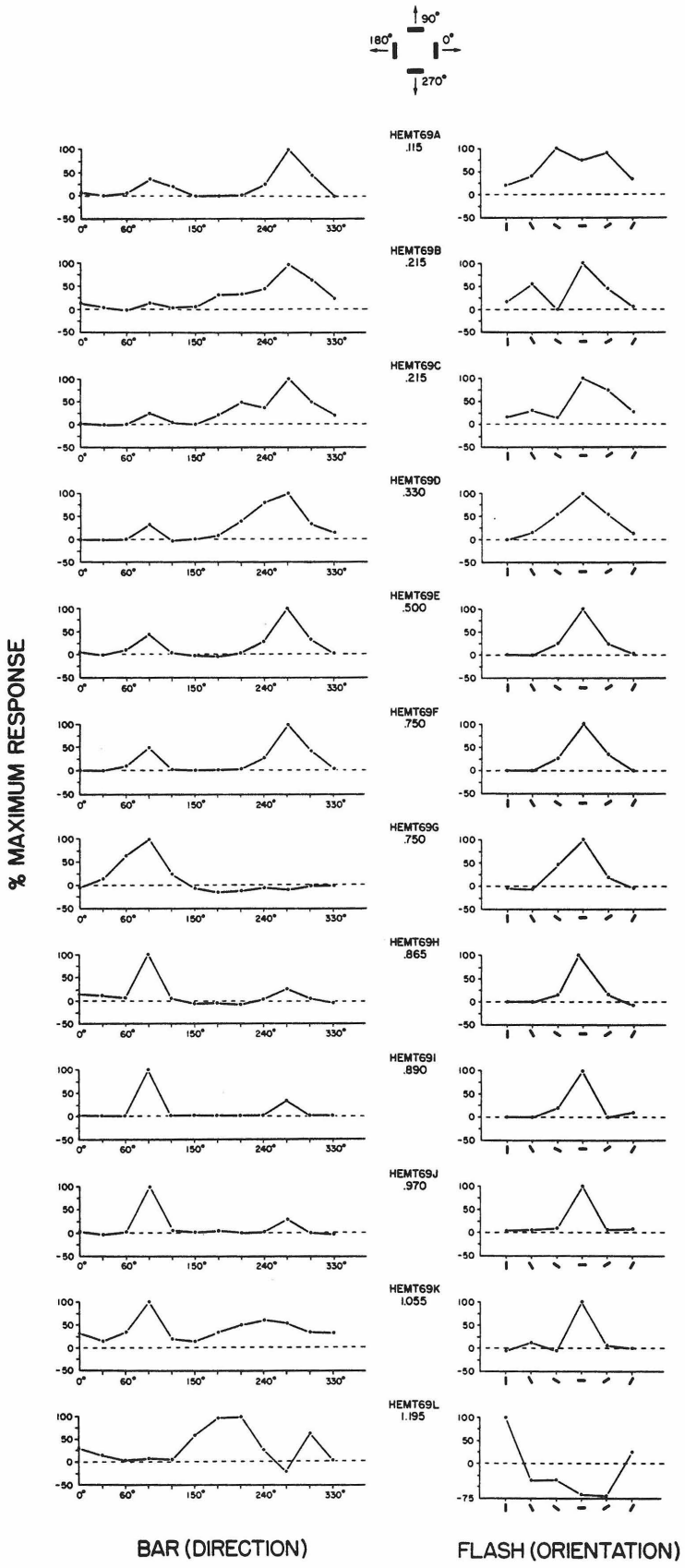
90°
180°
0°
270°
HEMT69A .115
HEMT69B .215
HEMT69C .215
HEMT69D .330
HEMT69E .500
HEMT69F .750
HEMT69G .750
HEMT69H .865
HEMT69I .890
HEMT69J .970
HEMT69K 1.055
HEMT69L 1.195
% MAXIMUM RESPONSE
BAR (DIRECTION)
FLASH (ORIENTATION)

was oriented perpendicular to the direction of movement. Neurons A through F responded optimally to a horizontally oriented bar approaching from 270° (straight down); neurons G through K responded optimally to a horizontally oriented bar approaching from 90° (straight up). One or more of these abrupt 180° shifts in preferred direction of movement have been observed in most of the long penetrations we have made in MT. These data suggest that groups of neurons with diametrically opposed preferred directions of movement lie juxtaposed within a larger system sharing the same orientation preference. We do not believe that the preferred direction is necessarily related to superficial versus deep layers, because we have observed other penetrations through all the layers in which all the cells had approximately the same preferred direction and orientation. While the preceding observations are generally characteristic of MT, some penetrations yielded less orderly patterns of organization.

The relative responsiveness to the array of randomly spaced dots was greater in the deep layers of MT, as demonstrated by the significant correlation between electrode depth in the cortex and the maximal responses obtained to the random dot array as a percentage of the best response to a bar stimulus ($r = 0.43$, $N = 31$, $p < 0.01$).

Eccentricity and receptive field size

The magnification of central vision differs widely across the extrastriate areas (1) and the distribution of eccentricities of single unit receptive fields from each area studied reflected the magnification in that area. The mean eccentricities (straight line distance from the center of gaze) of receptive field centers were: M, 36°; DM, 18°; DL, 13°; MT, 21°.

Extrastriate receptive fields varied widely in size and were generally much larger than striate fields (4). Excitatory receptive field areas were usually computed from elliptical mapped regions, although rarely an odd shape such as a very long

narrow rectangle or a kidney-shaped region was needed to accurately encompass the excitatory region. The mean receptive field areas were: M, 768^{o2} (sd = 919^{o2}); DM, 257^{o2} (sd = 737^{o2}); DL, 229^{o2} (sd = 297^{o2}); MT, 258^{o2} (sd = 371^{o2}). Receptive field area correlated well with eccentricity (r = 0.62 overall; M, r = 0.74; DM, r = 0.62; DL, r = 0.48; MT, r = 0.67). The large average receptive field size of M neurons could be partially explained by the peripheral location of receptive fields in M (8). Correlating eccentricity with the direction index (r = 0.07), tuning index (r = 0.17) and best velocity (r = 0.13) showed that the differences in response properties across the four areas could not be attributed to the eccentricity differences in the samples.

Summary comparison of response properties in DL, MT, DM, and M

A comparison of the functional indices for each area from this and related data from chapter II (60) are presented in Table 2. The high direction index for MT neurons compared with the significantly lower direction indices for DL, DM, and M indicates that MT neurons generally discriminate much better than cells in the other three areas the difference between movement in the preferred direction and movement in the direction 180° opposite. The orientation tuning index indicates that neurons in DM are significantly better tuned to the orientation of moving bars than in the other three areas, but the difference is small. In each of the four areas, the average tuning index for moving bars is lower than for stationary flashed bars. This implies that the response of a cell to moving oriented bars is some combination of a broadly-tuned response to direction of movement, and sharply tuned response to a stimulus' orientation. The random dot index indicates that MT neurons respond significantly better to the moving random dot array than do cells in DL and DM. The dimensional selectivity indices, which are explained fully in chapter II (60), indicate that DL neurons generally are significantly better tuned than neurons in the other three areas for stimuli of particular spatial dimensions.

TABLE 2

Comparison of response properties and central visual field representation in DL, MT, DM, and M.

The direction, orientation, and moving random dot indices are described in the text. The standard deviations for these indices are in the figures for each index. The dimensional selectivity index is taken from work published elsewhere (60). The index is calculated as: $1 - \frac{\text{response to longest stimulus tested}}{\text{response to optimal stimulus tested}}$. Length is the dimension orthogonal to the direction of movement. DL was also found to be significantly more selective for spot size than MT, DM, and M, and significantly more selective for width (dimension parallel to direction of movement) than MT (60). The percentage of each area devoted to the representation of the central 10° of the visual field was calculated from previous data (1, 3, 6-8).

Index	DL	MT	DM	M	Significant Differences
Directionality index (df=3,351)	.61	.81	.41	.37	MT> DL,DM,M
Orientation tuning (df-3,99)	.78	.85	.88	.80	none
Index for flashed bars					
Orientation tuning (df=3,351)	.50	.56	.67	.54	DM> MT,M,DL
Index for moving bars					
$\frac{\text{Best random dot response}}{\text{Best moving bar response}}$ (df=3,83)	.40	1.13	.25	.83	MT> DM,DL
Dimensional selectivity (df=3,94)	.59	.31	.28	.27	DL> MT,DM,M
Index for length					
Percentage of area devoted to central 10° of visual field	73%	10%	22%	4%	

DISCUSSION

Significance of multiple cortical areas

There is strong evidence that some aspects of the response properties of neurons are segregated in the four extrastriate areas studied. Why has functional localization of response properties taken place? In attempting to develop computer analogues of visual perception, Marr (48) elaborated the principle of modular design. Marr stated that any large computation should be broken into a collection of smaller modules as independent as possible from one another. Otherwise, "the process as a whole becomes extremely difficult to debug or improve, whether by a human designer or in the course of natural evolution, because a small change to improve one part has to be accompanied by many simultaneous changes elsewhere."

The formation of modules may have been produced by the replication of visual areas. The replication of existing structures appears to be a fumdamental mechanism in evolution. The paleontologist Gregory (29) proposed that a common mechanism of evolution is the replication of body parts due to genetic mutation in a single generation which is then followed in subsequent generations by the gradual divergence of structure and functions of the duplicated parts. The geneticist Bridges (13) proposed that chromosomal duplications would offer a reservoir of extra genes from which new ones might arise. It has been theorized that duplicated genes escape the pressures of natural selection operating on the original gene and thereby can accumulate mutations which enable the new gene, through changes in its DNA sequence, to encode for a novel protein capable of assuming new functions (57). Many clear-cut examples of gene replication have been discovered (39, 45, 57) and DNA sequence homologies in replicated genes have recently been established (64). The same evolutionary advantages which hold for the replication of genes may also hold for the replication of visual areas (3, 6).

What then are the likely modular functions of the extrastriate areas studied

here? Most neurons in all four areas are tuned for bar orientation as are the neurons in the primary visual cortex (37). This indicates that orientation selectivity is a main component of the basic plan for all the areas. MT neurons have supplemented this basic property of orientation selectivity with the further capability of discriminating direction of movement. This capacity is present in a minority of neurons in the other areas, but is much better developed in MT. In addition, MT has the capacity for discriminating an entirely different type of stimulus, moving arrays of random dots. In primary visual cortex in the cat, responsiveness to moving random dot arrays is characteristic of complex cells particularly in layer V, although these cells rarely respond better to visual texture than to an optimal bar as do the majority of cells in MT (33). This capacity to respond to random arrays requires a neural mechanism for integration over considerable distances in the visual cortex. A likely source of this integration is the convergence of input from primary visual cortex onto MT, particularly from the giant Meynert cells in layer V (52, 67; Wall, Lin and Kaas, personal communication). One of the outputs of MT is to the pontine nuclei (28), and this output is probably from the cells in the deep laminae, as is the case for the MT homologue in the macaque (26). Layer V corticopontine cells and pontine visual cells in the cat are similar to cells in the deep layers of MT; both are directionally selective and strongly respond to multiple spot stimuli (10, 24). The entire output of the pontine nuclei is to the cerebellum, a major center for the control of body and eye movement.

In DL about 70% of the neurons are selective for the spatial dimensions of visual stimuli within excitatory receptive fields that are generally much larger than the preferred stimulus dimensions (see Table 2). For details, see chapter II. The dimensional selectivity of DL neurons suggests that DL contributes to form perception. This hypothesis is consistent with the observation that DL has the most expanded representation of the central visual field (6) where the most acute

recognition of form takes place, and the recent discovery that DL is the main source of input to the inferotemporal cortex (84). Inferotemporal cortex has been strongly implicated in the analysis of complex visual stimuli and the learning of visual form discriminations (30, 31).

The most obvious distinctive feature of M is its relative emphasis on the representation of the peripheral visual field, which suggests that M might have a special role in functions in which peripheral vision is important, such as motion perception or orientation in space (8). However, the average direction index for area M neurons was the lowest of the four areas tested. DM is more sharply orientation selective when tested with moving bars than the other areas, but like the other areas is much less well tuned to moving bars than to flashed stationary bars. DM neurons were the least responsive to the moving array of random dots.

Homologies

There is abundant evidence for similarities between the organization of visual cortex in the owl monkey and in other primate species; in some cases these similarities are so striking that the areas in question should be considered to be homologous. The most widely quoted definition is that of Simpson (66): "homology is resemblance due to inheritance from common ancestry." Three major criteria for the recognition of homology in the nervous system proposed by Campbell and Hodos (15) are the multiplicity of similarities, the fineness of detail of the similarities, and evidence from fossil lineages of common ancestry.

The most powerful case for homology of the extrastriate visual areas is that of MT and similar visual areas in other primate species. This homology has been pointed out by several workers (31, 77, 78, 83). The argument for homology is based on similar location, myeloarchitecture, topography, distinctive anatomical connectivity, and visual response properties. Owl monkey MT is a striate-receptive region of dense myelination coextensive with an orderly map of the visual hemifield (3). A

corresponding striate-receptive region of dense myelination coextensive with a similar map of the visual field has been reported in Galago (9, 74), marmoset (68, 69), and macaque (23, 50, 80, 82). A major source of input to MT in the owl monkey is from V-I cells in or near the stria of Gennari and from the giant cells of Meynert located in the lower part of layer V (personal communication, Wall, Lin and Kaas). A similar projection occurs in marmoset (67) and macaque (46) from striate cortex cells in the stria of Gennari and the giant Meynert cells. MT is the only known extrastriate cortical target of the Meynert cells (47). Directional selectivity is the principal characteristic of owl monkey MT cell responses, and this has been shown to be true for the corresponding region of the macaque (50, 89). The presence of these extensive and detailed similarities in three superfamilies of primates, including primates from both infraorders, indicates that MT probably existed in the early primates ancestral to all living primates.

In a recent paper, Zeki (92) contends that MT in the owl monkey and the striate projection zone of the superior temporal sulcus in the macaque are not homologous. However, Zeki's discussion of structural similarities does not include any mention of the distinctive heavy myelination of the deeper layers of owl monkey and macaque MT, nor does he mention the precise similarity in anatomical projection to MT from striate cortex. While Zeki found that owl monkey MT cells shared with macaque MT cells the major property of directional selectivity, his argument rests primarily on his contention that there are major differences in the visual response properties of owl monkey and macaque MT cells. He cites three differences: a) the dependence of owl monkey MT cell responses on the presence of a near optimal stimulus and the relative absence of such dependence in the macaque, b) the presence of orientation selectivity in most owl monkey MT cells and its relative rarity in macaque MT cells, and c) the presence of a wide variety of binocular interaction effects on owl monkey MT cells but not on macaque cells.

Zeki states that the stimulus requirements of owl monkey MT cells "made the initial penetrations frustrating, with cell after cell either not responding, or responding in a vague manner." This was not the case under our experimental conditions. While we found many examples of orientation, length, width, and/or diameter selectivity (59), we also found in the same cells that any of a wide variety of non-optimal, non-oriented stimuli evoked vigorous responses and these responses had impressive signal-to-noise ratios. In fact, a field of randomly scattered dots was the optimal stimulus for the majority of MT cells, and most cells were also well driven by a single spot (see Table 1). This contradiction between our results and Zeki's may be due to differences between the two preparations, possibly the use of vetame-ketamine tranquilization versus barbiturate anesthesia. The results of our flashed oriented bar presentations clearly support Zeki's claim of orientation selectivity in owl monkey MT cells. However, we do not know whether orientation selectivity would be revealed in macaque MT with the flashed bar test, and without a description of Zeki's orientation selectivity testing procedure, it is difficult to evaluate the differences he reports. In both owl monkey MT and the striate projection zone in the superior temporal sulcus of the macaque, Zeki found the majority of cells to be driven equally by stimulation of either eye. The presence of a minority of cells having more specialized binocular interactions in the owl monkey MT suggests a greater emphasis on binocular processing.

In our present state of knowledge, it is more difficult to establish clear-cut homologies for the other visual areas found beyond V-II in the owl monkey. However, evidence for the homology of several areas is emerging. The principal input to inferotemporal visual cortex in the owl monkey is DL (84). In macaques a region adjacent to MT is a main input to inferotemporal cortex (20). This region, like DL in the owl monkey, emphasizes the representation of the central visual field (21). MT in both owl monkeys and macaques does not appear to project to inferotemporal cortex.

The position of DL between MT and V-II in owl monkeys is topographically similar to V-4 in macaques. However, the boundaries of V-4 have not been completely mapped, and it may constitute more than one area (80, 88). Neurons in V-4 have been reported to be color selective, but the percentage of neurons showing this attribute in V-4 has ranged from 100% to 32% in different studies, and a recent report suggests that color processing in V-4 is substantially similar to the color selectivity found in foveal V-I and V-II (43).

Another potential homology is that of the Ventral Posterior (VP) areas of the owl monkey and the macaque (54, 56, see Fig. 1). These areas are similar in that they both are long narrow strips that lie immediately anterior to V-II on the ventral surface, with this common border corresponding to a representation of the horizontal meridian. In both monkeys, the anterior border of VP corresponds to a discrete band of degeneration following section of the corpus callosum. In both monkeys, the visual field representation in VP appears to be limited to the upper quadrant with the more central portions represented laterally and the more peripheral portions medially. The establishment of potential homologies for DM and M awaits further investigation.

Outside of primates it is much more difficult to establish homologies. The last common ancestor of the different mammalian orders lived no more recently than the late Cretaceous period more than 60 million years ago (63). This ancestral mammal had only a very limited development of its neocortex (40). In addition, the adaptive radiation of mammals into different ecological niches with widely divergent behavioral specializations serves to make very difficult the discovery of diagnostic similarities among potentially homologous cortical areas in different mammalian orders.

In the cat, area 21a and area 19 (V-3) occupy positions that bear some topographic similarities to MT and DL; area 19 partially wraps around area 21a, and the two areas adjoin each other along a common border representing the vertical

meridian in the lower field (76). The dimensionally selective properties of DL neurons resemble some of the higher-order-hypercomplex cells described by Hubel and Wiesel for V-III in the cat, although these cells were only a small portion of their sample (35). Area 21a, while bearing some topographic similarity to MT, contains a representation of only the central 30° of the contralateral hemifield. The striate-receptive lateral suprasylvian region in the cat has been suggested as a potential homologue of MT (1). The neurons in the lateral suprasylvian region typically are directionally selective and thus resemble MT in this respect (36, 71). The neurons have also been reported to have dimensionally selective properties similar to DL (14). The establishment of homologies with this region in the cat is further complicated by the recent discovery that it contains six visual areas (58).

In the grey squirrel, the temporal posterior area (Tp) is a possible homologue of MT. Tp lies adjacent to part of the vertical meridian representation in area 19, and thus these areas bear a topographic similarity to MT and DL (32). In addition, Tp, like MT, is densely myelinated with a laminar pattern similar to MT (41). In a similar location in the rabbit, there is a striate-receptive visual area that has been suggested as a possible homologue of MT, but the response properties of the nuerons in this area in the rabbit differ markedly from MT (17, 49).

While similarities in the organization of other mammals is less well documented, multiple representations of the visual field exist in many other species (78). Multiple representations also occur in other sensory systems, for example the auditory (38), and somatosensory (51, see Fig. 1). The ubiquitous nature of multiple representations, and the evidence for the localization of response properties to these areas argues that functional localization is a successful evolutionary solution to the problems of complex information processing.

REFERENCES

1. Allman, J. M. Evolution of the visual system in the early primates. In: Progr. Psychobiol. Physiol. Psych., Vol. **7**, edited by J. M. Sprague and A. N. Epstein. New York Academic Press, 1977.
2. Allman, J. M., Campbell, C. B. G. and McGuinness, E. The dorsal third tier area in Galago senegalensis. Brain Res. **179:** 355-361, 1979.
3. Allman, J. M. and Kaas, J. H. A representation of the visual field in the caudal third of the middle temporal gyrus of the owl monkey (Aotus trivirgatus). Brain Res. **31:** 84-105, 1971a.
4. Allman, J. M. and Kaas, J. H. Representation of the visual field in striate and adjoining cortex of the owl monkey (Aotus trivirgatus). Brain Res. **35:** 89-106, 1971b.
5. Allman, J. M. and Kaas, J. H. The organization of the second visual area (VII) in the owl monkey: A second order transformation of the visual hemifield. Brain Res. **76:** 247-265, 1974a.
6. Allman, J. M. and Kaas, J. H. A crescent-shaped cortical visual area surrounding the middle temporal area (MT) in the owl monkey (Aotus trivirgatus). Brain Res. **81:** 199-213, 1974b.
7. Allman, J. M. and Kaas, J. H. The dorsomedial cortical visual area: A third tier area in the occipital lobe of the owl monkey (Aotus trivirgatus). Brain Res. **100:** 473-487, 1975.
8. Allman, J. M. and Kaas, J. H. Representation of the visual field on the medial wall of occipital-parietal cortex in the owl monkey. Science **191:** 572-575, 1976.
9. Allman, J. M., Kaas, J. H. and Lane, R. H. The middle temporal visual area (MT) in the bushbaby, Galago senegalensis. Brain Res. **57:** 197-202, 1973.
10. Baker, J. F., Gibson, A., Glickstein, G. and Stein, J. Visual cells in the pontine nuclei of the cat. J. Physiol., London **255:** 415-433, 1976.

11. Baker, J. F., Petersen, S. E., Newsome, W. T. and Allman, J. M. Visual response properties of neurons in four extrastriate visual areas of the owl monkey (Aotus trivirgatus): a quantitative comparison of Medial, Dorsomedial, Dorsolateral and Middle Temporal areas. J. Neurophysiol. **45:** 397-416, 1981.

12. Barlow, H. B., Hill, R. M. and Levick, W. R. Retinal ganglion cells responding selectively to direction and speed of image motion in the rabbit. J. Physiol., London **173:** 377-407, 1964.

13. Bridges, C. B. Salivary chromosome maps. J. Hered. **26:** 60-64, 1935.

14. Camarda, R. and Rizzolatti, G. Visual receptive fields in the lateral suprasylvian area (Clare-Bishop area) of the cat. Brain Res. **101:** 427-443, 1976.

15. Campbell, C. B. G. and Hodos, W. The concept of homology and the evolution of the nervous system. Brain Behav. Evol. **3:** 353-367, 1970.

16. Chan-Palay, V., Palay, S. L. and Billings-Gagliardi, S. M. Meynert cells in the primate visual cortex. J. Neurocytol. **3:** 631-658, 1974.

17. Chow, K. L., Douville, A., Muscetti, G. and Grobstein, P. Receptive field characteristics of neurons in a visual area of the rabbit temporal cortex. J. Comp. Neurol. **171:** 135-146, 1976.

18. Cragg, B. G. The topography of the afferent projections in circumstriate visual cortex of the monkey studied by the Nauta method. Vision Res. **9:** 733-747, 1969.

19. Cynader, M. and Berman, N. Receptive field organization of monkey superior colliculus. J. Neurophysiol. **35:** 187-201, 1972.

20. Desimone, R., Fleming, J. and Gross, C. G. Prestriate afferents to inferior temporal cortex: an HRP study. Brain Res., in press, 1980.

21. Desimone, R. and Gross, C. G. Visual areas in the temporal cortex of the macaque. Brain Res. **178:** 363-380, 1979.

22. Fernald, R. and Chase, R. An improved method for plotting retinal landmarks and focusing the eyes. Vision Res. **11:** 95-96, 1971.

23. Gattas, R. and Gross, C. G. A visuotopically organized area in the posterior superior temporal sulcus of the macaque. ARVO Annual Meeting Abstr., 1979, p. 184.

24. Gibson, A., Baker, J., Mower, G. and Glickstein, M. Corticopontine cells in area 18 of the cat. J. Neurophysiol. **41:** 484-495, 1978.

25. Gilbert, C. D. and Kelly, J. P. The projections of cells in different layers of the cat's visual cortex. J. Comp. Neurol. **163:** 81-105, 1975.

26. Glickstein, M., Cohen, J., Dixon, B., Gibson, A., Hollins, M., La Bossiere, E. and Robinson, F. Corticopontine visual projection in the macaque monkey. J. Comp. Neurol. **180:** 209-230, 1980.

27. Goldberg, M. E. and Wurtz, R. H. Activity of superior colliculus in behaving monkey. I. Visual receptive fields of single neurons. J. Neurophysiol. **35:** 542-559, 1972.

28. Graham, J., Lin, C.-S. and Kaas, J. H. Subcortical projections of six visual cortical areas in the owl monkey, Aotus trivirgatus. J. Comp. Neurol. **187:** 557-580, 1979.

29. Gregory, W. K. Reduplication in evolution. Quart. Rev. Biol. **10:** 272-290, 1935.

30. Gross, C. G. Visual functions of inferotemporal cortex. In: Handbook of Sensory Physiology V11/3 B, edited by R. Jung. Berlin: Springer, 1973, p. 451-482.

31. Gross, C. G., Bruce, C. J., Desimone, R., Fleming, J. and Gattas, R. Three visual areas of the temporal lobe. In: Multiple Cortical Areas, edited by C. N. Woolsey. Englewood Cliffs, New Jersey: Humana Press, in press, 1980.

32. Hall, W. C., Kaas, J. H., Killackey, H. and Diamond, I. T. Cortical visual areas in the grey squirrel (Sciurus carolinensis): A correlation between cortical evoked potential maps and architectonic subdivisions. J. Neurophysiol. **34:** 437-452, 1971.

33. Hammond, P. and MacKay, D. M. Differential responsiveness of simple and complex cells in cat striate cortex to visual texture. Exptl. Brain Res. **30:** 106-154, 1977.

34. Hubel, D. H. and Wiesel, T. N. Receptive fields, binocular interaction and functional architecture in the cat's visual cortex. J. Physiol., London **160:** 106-154, 1962.

35. Hubel, D. H. and Wiesel, T. N. Receptive fields and functional architecture in two non-striate visual areas (18 and 19) of the cat. J. Neurophysiol. **28:** 229-289, 1965.

36. Hubel, D. H. and Wiesel, T. N. Visual area of the lateral suprasylvian gyrus (Clare-Bishop area) of the cat. J. Physiol., London **202:** 251-260, 1969.

37. Hubel, D. H. and Wiesel, T. N. Functional architecture of macaque monkey visual cortex. Proc. Roy. Soc. B **198:** 1-59, 1977.

38. Imig, T. J., Ruggero, M. A., Kitzes, L. M., Javel, E. and Brugge, J. F. Organization of auditory cortex in the owl monkey (Aotus trivirgatus). J. Comp. Neurol. **171:** 111-128, 1977.

39. Ingram, V. M. The Hemoglobins in Genetics and Evolution. New York: Columbia Univ. Press, 1963.

40. Jerison, H. Evolution of the Brain and Intelligence. New York: Academic Press, 1973.

41. Kaas, J. H., Hall, W. C. and Diamond, I. T. Visual cortex of the grey squirrel (Sciurus carolinensis): Architectonic subdivisions and connections from the visual thalamus. J. Comp. Neurol. **145:** 273-306, 1972.

42. Kadoya, S., Wolin, L. R. and Massopust, L. C. Photically evoked unit activity in the tectum opticum of the squirrel monkey. J. Comp. Neurol. **158:** 319-338, 1972.

43. Kruger, J. and Gouras, P. Spectral selectivity of cells and its dependence on slit length in monkey visual cortex. J. Neurophysiol. **43:** 1055-1069, 1980.

44. Kuypers, H. G. J. M., Szwarcbart, M. K., Mishkin, M. and Rosvold, H. E. Occipito-temporal cortico-cortical connections in the rhesus monkey. Exptl. Neurol. **11:** 245-262, 1965.

45. Lewis, E. B. Pseudoallelism and gene evolution. Cold Spring Harbor Symp. Quant. Biol. **16:** 159-174, 1951.

46. Lund, J. S., Lund, R. D., Hendrickson, A. E., Bunt, A. H. and Fuchs, A. F. The origin of efferent pathways from the primary visual cortex, area 17, of the macaque monkey as shown by retrograde transport of horseradish peroxidase. J. Comp. Neurol. **164:** 287-304, 1976.

47. Lund, J. S., Henry, G. H., MacQueen, C. L. and Harvey, A. R. Anatomical organization of the primary visual cortex (area 17) of the cat. A comparison with area 17 of the macaque monkey. J. Comp. Neurol. **184:** 599-618, 1979.

48. Marr, D. Early processing of visual information. Phil. Trans. Roy. Soc., London, Series B **275:** 484-519, 1976.

49. Mathers, L. H., Douville, A. and Chow, K. L. Anatomical studies of a temporal visual area in the rabbit. J. Comp. Neurol. **171:** 147-156, 1977.

50. Maunsell, J. H. R., Bixby, J. L. and Van Essen, D. C. The middle temporal (MT) area in the macaque: Architecture, functional properties and topographic organization. Soc. Neurosci. Abstr. **5:** 796, 1980.

51. Merzenich, M. M., Kaas, J. H., Sur, M. and Lin, C.-S. Double representation of the body surface within cytoarchitectonic areas 3b and 1 in SI in the owl monkey (Aotus trivirgatus). J. Comp. Neurol. **181:** 41-74, 1978.

52. Montero, V. M. Patterns of connections from the striate cortex to cortical visual areas in superior temporal sulcus of macaque and middle temporal gyrus of owl monkey. J. Comp. Neurol. **189:** 45-55, 1980.

53. Myers, R. E. Commissural connections between occipital lobes of the monkey. J. Comp. Neurol. **118:** 1-16, 1962.

54. Newsome, W. T. and Allman, J. M. The interhemispheric connections of visual cortex in the owl monkey, Autus trivirgatus, and the bushbaby, Galago senegalensis. J. Comp. Neurol. **194:** 209-233, 1980.

55. Newsome, W. T., Baker, J. F., Miezin, F. M., Myerson, J., Petersen, S. E. and Allman, J. M. Functional localization of neuronal response properties in extrastriate visual cortex of the owl monkey. ARVO Annual Meeting Abstr., 1978, p. 174.

56. Newsome, T. W., Maunsell, J. H. R. and Van Essen, D. C. Areal boundaries and topographic organization of the ventral posterior area (VP) of the macaque monkey. Soc. Neurosci. Abstr. **6:** 599, 1980.

57. Ohno, S. Evolution by Gene Duplication. New York: Spring, 1970, pp. 1-160.

58. Palmer, L. A., Rosenquist, A. C. and Tusa, R. J. The retinotopic organization of lateral suprasylvian visual areas in the cat. J. Comp. Neurol. **177:** 237-256, 1978.

59. Petersen, S. E., Baker, J. F., Rockland, K. S. and Allman, J. M. Visual response properties of single neurons in the dorsolateral crescent (DL) in the owl monkey: selectivity for stimulus size, direction, and orientation. Soc. Neurosci. Abstr. **5:** 579, 1980.

60. Petersen, S. E., Baker, J. F. and Allman, J. M. Dimensional selectivity of neurons in the dorsolateral visual area of the owl monkey. Brain Res. **197:** 507-511, 1980.

61. Pettigrew, J. D., Nikara, T. and Bishop, P. O. Responses to moving slits by single units in cat striate cortex. Exptl. Brain Res. **6:** 373-390, 1968.

62. Pollard, J. H. A Handbook of Numerical and Statistical Techniques. Cambridge: Cambridge Univ. Press, 1977.

63. Romer, A. S. Vertebrate Paleontology. Chicago: Univ. of Chicago Press, 1966, pp. 1-460.

64. Royal, A., Garapin, A., Cami, B., Perrin, F., Mandel, J. L., LeMeur, M., Brégégègre, F., Gannon, F., LePennec, J. P., Chambon, P. and Kourilsky, P. The ovalbumin gene region: common features in the organization of three genes expressed in chicken oviduct under hormonal control. Nature **279:** 125-132, 1979.

65. Schiller, P. H. and Koerner, F. Discharge characteristics of single units in superior colliculus of the alert rhesus monkey. J. Neurophysiol. **34:** 920-936, 1971.

66. Simpson, G. G. Principles of Animal Taxonomy. New York: Columbia Univ. Press, 1961.

67. Spatz, W. B. An efferent connection of the solitary cells of Meynert. A study with horseradish peroxidase in the marmoset, Callithrix. Brain Res. **92:** 450-455, 1975.

68. Spatz, W. B. Topographically organized reciprocal connections between areas 17 and MT (visual area of the superior temporal sulcus) in the marmoset (Callithrix jacchus). Exptl. Brain Res. **27:** 559-572, 1977.

69. Spatz, W. B. and Tigges, J. Experimental-anatomical studies on the "Middle Temoporal Visual Area (MT)" in primates. I. Efferent cortico-cortical connections in the marmoset (Callithrix jacchus). J. Comp. Neurol. **146:** 451563, 1972.

70. Spatz, W. B., Tigges, J. and Tigges, M. Subcortical projections, cortical associations, and some intrinsic interlaminar connections of the striate cortex in the squirrel monkey (Saimiri). J. Comp. Neurol. **140:** 155-174, 1970.

71. Spear, P. D. and Baumann, T. P. Receptive-field characteristics of single neurons in lateral suprasylvian visual area of the cat. J. Neurophysiol. **38:** 1403-1420, 1975.

72. Sterling, P. and Wickelgren, B. G. Visual receptive fields in the superior colliculus of the cat. J. Neurophysiol. **32:** 1-15, 1969.

73. Talbot, S. A. A lateral localization in cat's visual cortex. Fed. Proc. **1:** 84, 1942.

74. Tigges, J., Tigges, M. and Kalaha, C. S. Efferent connections of area 17 in Galago. Am. J. Phys. Anthropol. **38:** 393-398, 1973.

75. Tusa, R. J., Palmer, L. A. and Rosenquist, A. C. The retinotopic organization of the visual cortex in the cat. Soc. Neurosci. Abstr. **5**, 1972, p. 52.

76. Tusa, R. J. and Palmer, L. A. The retinotopic organization of areas 20 and 21 in the cat. J. Comp. Neurol., in press, 1980.

77. Ungerleider, L. G. and Mishkin, M. The striate projection zone in the superior temporal sulcus of Macaca mulatta: Location and topographic organization. J. Comp. Neurol. **188:** 347-366, 1979.

78. Van Essen, D. C. Visual cortical areas. In: Ann. Rev. Neurosci., Vol. 2, edited by W. M. Cowan. Palo Alto: Annual Reviews, Inc., 1979, pp. 227-263.

79. Van Essen, D. C., Maunsell, J. H. R. and Bixby, J. L. The organization of extra-striate visual areas in the macaque monkey. In: Multiple Cortical Areas, edited by C. N. Woolsey. Englewood Cliffs, New Jersey: Humana Press, in press, 1980.

80. Van Essen, D. C. and Zeki, S. M. The topographic organization of rhesus monkey prestriate cortex. J. Physiol., London **277:** 193-226, 1978.

81. Watkins, D. W., Wilson, J. R., Sherman, S. M. and Berkley, M. A. Receptive field organization: further differences between simple and complex cells. ARVO Annual Meeting Abstr., 1975, p. 17.

82. Weller, R. E. and Kaas, J. H. Connections of striate cortex wtih the posterior bank of the superior temporal sulcus in macaque monkeys. Soc. Neurosci. Abstr., 1978, p. 650.

83. Weller, R. E. and Kaas, J. H. Cortical and subcortical connections of visual cortex in primates. In: Multiple Cortical Areas, edited by C. N. Woolsey. Englewood Cliffs, New Jersey: Humana Press, 1980a, in press.

84. Weller, R. E. and Kaas, J. H. Connections of the dorsolateral visual area (DL) of extrastriate visual cortex of the owl monkey (Aotus trivirgatus). Soc. Neurosci. Abstr. **6:** 580, 1980.

85. Wolbarsht, M. L., MacNichol, E. F. and Wagner, H. G. Glass insulated platinum microelectrode. Science **132:** 1309-1310, 1960.

86. Wright, M. J. Visual receptive fields of cells in a cortical area remote from the striate cortex of the cat. Nature **223:** 973-975, 1969.

87. Zeki, S. M. Representation of central visual fields in prestriate cortex of monkey. Brain Res. **14:** 271-291, 1969.

88. Zeki, S. M. Colour coding in the superior temporal sulcus of rhesus monkey visual cortex. Brain Res. **53:** 422-427, 1973.

89. Zeki, S. M. Functional organization of a visual area in the posterior bank of the superior temporal sulcus of the rhesus monkey. J. Physiol., London **236:** 549-573, 1974.

90. Zeki, S. M. Uniformity and diversity of structure and function in rhesus monkey prestriate cortex. J. Physiol., London **277:** 273-290, 1978.

91. Zeki, S. M. Functional specialization in the visual cortex of the rhesus monkey. Nature **274:** 423-428, 1978.

92. Zeki, S. M. The response properties of cells in the middle temporal area (area MT) of owl monkey visual cortex. Proc. Roy. Soc. London B **207:** 239-248, 1980.

Chapter 2

DIMENSIONAL SELECTIVITY OF EXTRASTRIATE NEURONS

INTRODUCTION

As was noted in Chapter 1, one of the extrastriate areas, the dorsolateral crescent visual area, DL, has an extreme magnification, or overrepresentation, of the central portions of the visual field. This magnification of the center of vision suggests that DL contributes to the analysis of form, since it is at the center of gaze that the most critical analysis of form takes place. A simple and easily measurable aspect of the form of a visual stimulus is its size. We tested the neurons of the dorsolateral crescent for length, width, and spot diameter selectivity, and found that a high percentage of neurons in that area are selective for the spatial dimensions of visual stimuli within excitatory receptive fields much larger than the preferred stimulus dimensions. In preliminary results from three other extrastriate areas, such neurons are much less common. In Chapter 2, the properties of the dimensional selectivity of DL neurons are reported, and their properties are compared with similar neuronal response properties in other species.

METHODS

Single neurons were recorded from four extrastriate areas of two chronically-prepared owl monkeys. One hundred nine neurons were studied quantitatively (52 from DL; 30 from the middle temporal area, MT; 13 from the dorsomedial area, DM; 14 from the medial area, M. Recording techniques were identical to those described in Chapter 1. To test for dimensional selectivity, the computer presented stimuli in pseudorandomly-ordered sequences of bars of various lengths (the dimension orthogonal to the direction of motion), widths (the dimension parallel to the direction of motion), and spots of various diameters. All spike information was computer-collected and stored on magnetic disk for later analysis. Response magnitude was calculated as the difference between the mean impulse rate during the stimulus presentation and the mean spontaneous rate. Nearly all extrastriate neurons

Figure 1. Responses of 3 units to different bar lengths. Length is the stimulus dimension perpendicular to the direction of movement; stimuli were oriented at 90° to the direction of movement and were 1° wide. The value at each length is the average of 5 stimuli. Lengths were presented in pseudorandom order. The upper two cells were recorded from DL and show marked length selectivity. The length of the excitatory receptive field for the top cell was 27° and for the middle cell, 20°. The bottom cell illustrates the typical response profile for cells in MT, DM, and M, in which the cell summates with increasing length until the length of the excitatory receptive field is reached, whereupon the response levels off.

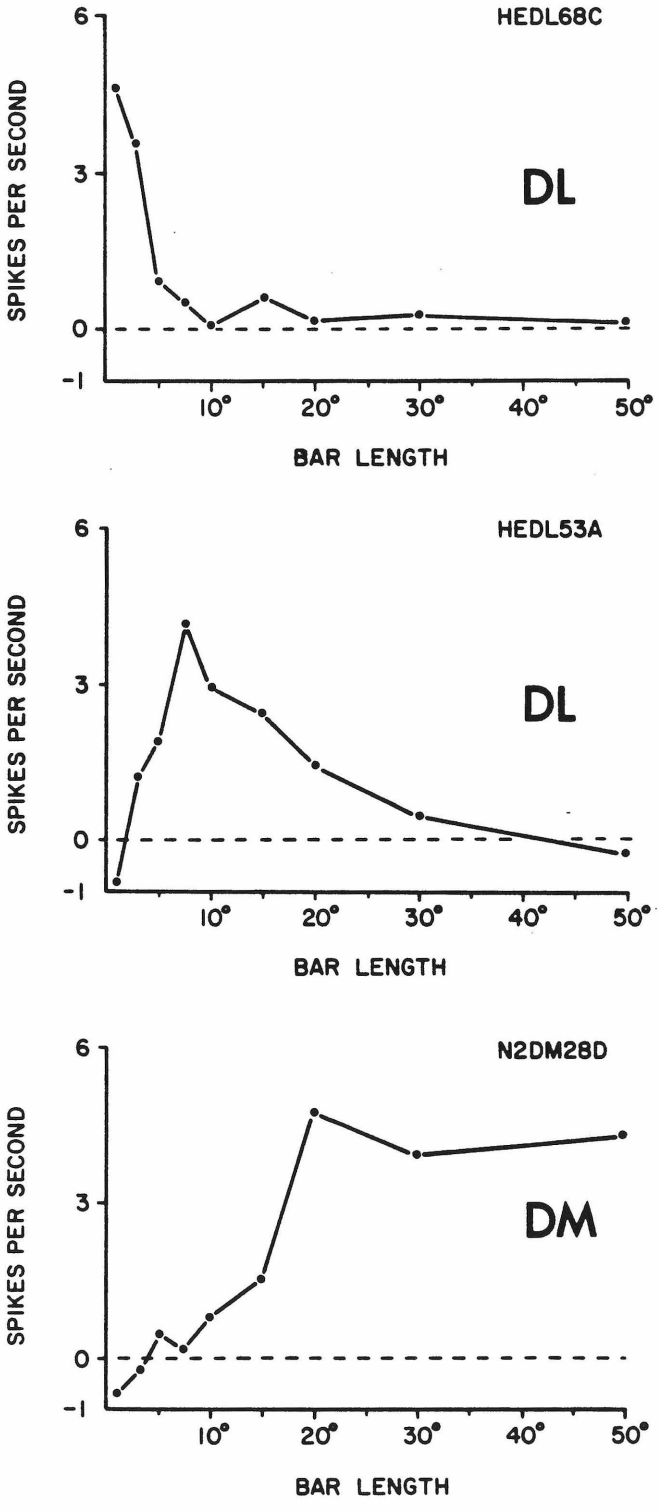
HEDL68C
DL
SPIKES PER SECOND
6
3
0
-1
10°
20°
30°
40°
50°
BAR LENGTH
HEDL53A
DL
SPIKES PER SECOND
6
3
0
-1
10°
20°
30°
40°
50°
BAR LENGTH
N2DM28D
DM
SPIKES PER SECOND
6
3
0
-1
10°
20°
30°
40°
50°
BAR LENGTH

exhibited some direction, orientation and velocity sensitivity (see Chapter 1), and the dimension series were run at the optimal velocity in the preferred direction for each neuron studied.

RESULTS

Most DL neurons were sharply dimensionally selective; they responded well only to stimuli which had near optimal dimensions (see Fig. 1a and 1b). Most cells outside of DL showed response summation up to a certain stimulus value, but were unaffected by further increases (Fig. 1c). An index of stimulus dimension selectivity was calculated using the formula:

$$DI = 1 - \frac{\text{response to the largest stimulus dimension tested}}{\text{response to the optimal stimulus dimension tested}}$$

For length and spot diameter, DL cells were significantly more selective than cells in DM, M, and MT, and were significantly more selective for width than MT neurons. The statistical test used was a one-way analysis of variance with comparisons being made between areas using Scheffe's multiple comparisons (see Fig. 2 for S-values) (14). We assumed that recordings made in the same area of different animals were from the same population. Figures 2a, 2b and 2c are the distribution of selectivity indices for the four areas.

The dimensional selectivity of DL cells was independent of the amount or sign of contrast in the receptive field. Eight cells which responded well to either contrast were tested using both light-on-dark and dark-on-light stimuli, and the results were invariably similar (Fig. 3). Varying stimulus contrast over a 1.5 log unit range likewise had little effect on a unit's responsiveness.

The optimal length and width were typically considerably smaller than the mapped excitatory receptive field. This is illustrated in Figs. 4a and 4b which are distributions of optimal lengths as a proportion of receptive field length. Cells which

Figure 2. Distributions of stimulus dimension selectivity indices for length (A), width (B), and spot diameter (C). The distributions for DL cells are on the left, and the distributions for MT, M, and DM cells are on the right. Statistics comparing these distributions; df for length = 3, 94; width = 3, 36; spot diameter = 3, 81. S-values for length, width and spot diameter selectivity, respectively: DL vs MT = 3.42*, 3.91*, 8.66*; DL vs M = 3.14*, 1.53, 3.44*; DL vs DM = 2.76*, 1.55, 4.94*; MT vs M = 0.05, 0.21, 0.29; MT vs DM = 0.03, 0.07, 0.01; M vs DM = 0.01, 0.02, 0.21.

*means p less than 0.05.

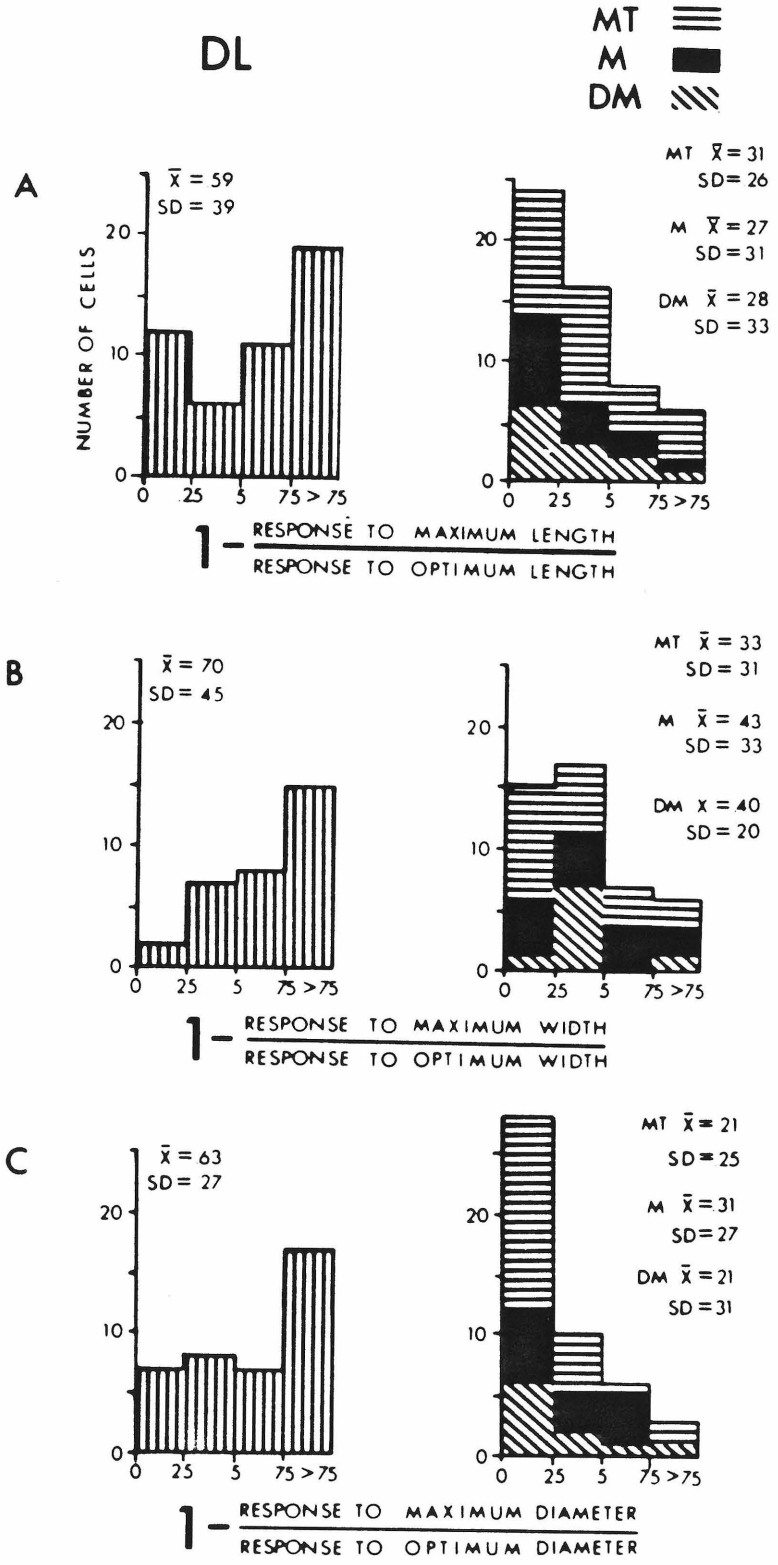
DL
MT
M
DM
A
$\bar{x}$ = 59
SD = 39
NUMBER OF CELLS
MT $\bar{x}$ = 31
SD = 26
M $\bar{x}$ = 27
SD = 31
DM $\bar{x}$ = 28
SD = 33
0 25 5 75 > 75
1 − RESPONSE TO MAXIMUM LENGTH / RESPONSE TO OPTIMUM LENGTH
B
$\bar{x}$ = 70
SD = 45
MT $\bar{x}$ = 33
SD = 31
M $\bar{x}$ = 43
SD = 33
DM x = 40
SD = 20
1 − RESPONSE TO MAXIMUM WIDTH / RESPONSE TO OPTIMUM WIDTH
C
$\bar{x}$ = 63
SD = 27
MT $\bar{x}$ = 21
SD = 25
M $\bar{x}$ = 31
SD = 27
DM $\bar{x}$ = 21
SD = 31
1 − RESPONSE TO MAXIMUM DIAMETER / RESPONSE TO OPTIMUM DIAMETER

Figure 3. Responses of a DL neuron to light and dark spots of different diameters. Receptive field position is shown above. The stimuli were presented in pseudorandom order. Responses to stimuli of the same size were virtually the same regardless of contrast.

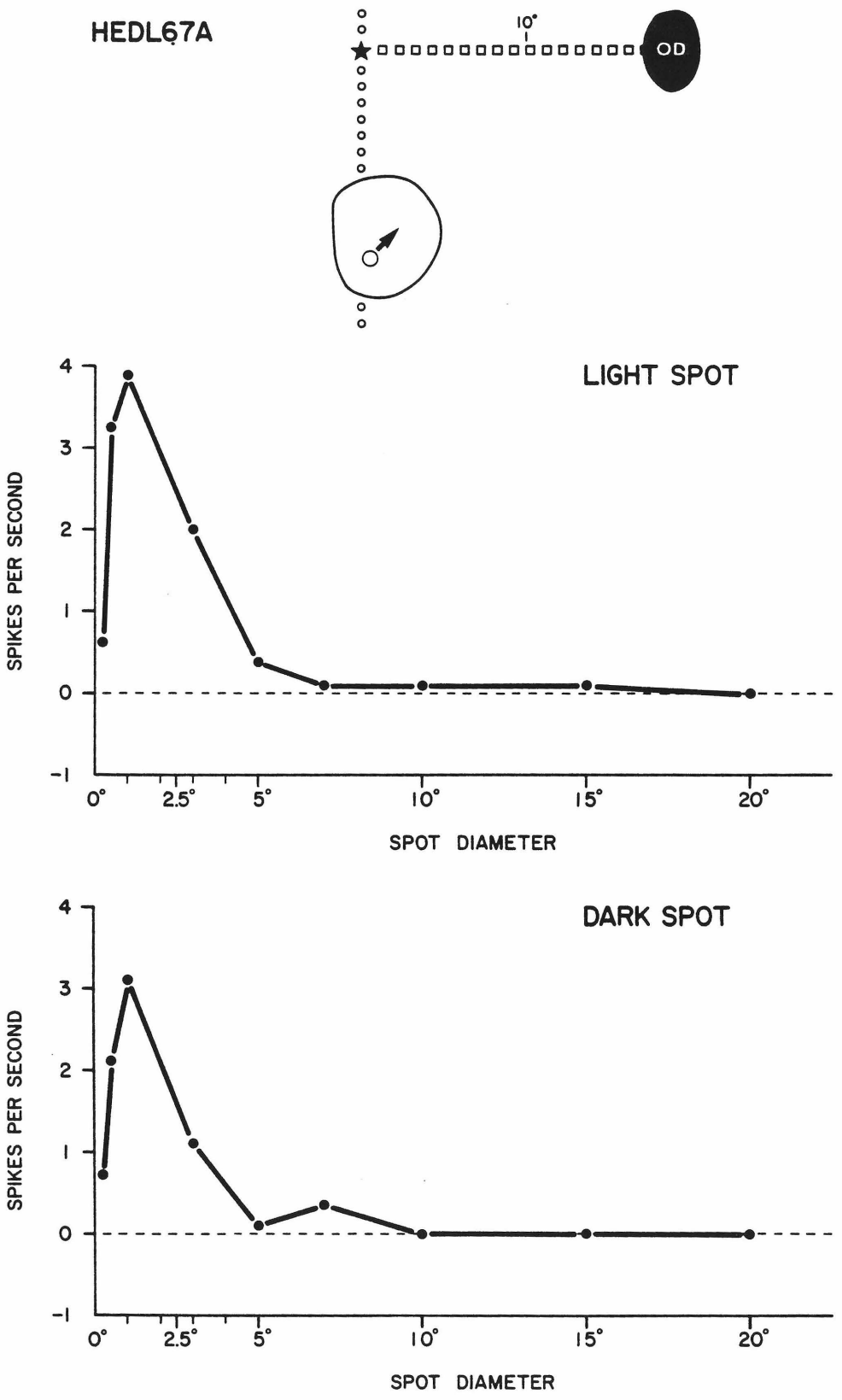
HEDL67A
10°
OD
LIGHT SPOT
SPIKES PER SECOND
4
3
2
1
0
-1
0°
2.5°
5°
10°
15°
20°
SPOT DIAMETER
DARK SPOT
SPIKES PER SECOND
4
3
2
1
0
-1
0°
2.5°
5°
10°
15°
20°
SPOT DIAMETER

had a selectivity index of 0.5 or less were considered as non-selective and are represented in the columns at the right. The dimensional selectivity of DL cells was also independent of stimulus position in the excitatory receptive field.

DL neurons had a wide range of optimal stimulus dimensions. The length and width preferences appeared independent of each other for 21 cells in which both dimensions were tested. Although, as shown in Fig. 5, a 1 degree square was the most frequently encountered optimal stimulus, the figure clearly demonstrates that dimensionally-selective DL cells are not spot detectors tuned to different diameters but are selective for the shape of the stimulus in both dimensions. Of the 17 cells in DL from which complete data for all three spatial tests were available, 14 responded better to the best rectangular stimulus than to the best spot.

DISCUSSION

Many examples of cells sensitive to the spatial dimensions of visual stimuli have been reported. These reports are summarized in Table 1. In some cases, the cells exhibit profound differences from the cells found in DL. The cells in the rabbit temporal lobe (5), and the convex edge detectors in the frog optic nerve and tectum (13) are not independent of contrast, in that they fire only to dark-on-light stimuli. The local edge detectors in the cat and rabbit retinae (6, 13), the spot cells in V-II of the macaque (2), and the convex edge detectors of the frog are strongly dependent on the position of the stimulus in the receptive field. Most of these cells, including the neurons in the superficial layers of the superior colliculus in the macaque (15), lack the orientation and direction specificity of the DL neurons, and the DL cells' independent specification of length and width. One type of higher order hypercomplex cell (see ref. 10, Figs. 23-25) found in V-III of the cat closely corresponds to the neurons found in DL. However, we have found no evidence, other than the DL cells' preference for rectangular stimuli, that the cells show the characteristic higher

Figure 4. Optimal bar length compared with receptive field length for DL, DM, MT, and M. Optimal bar length is expressed as a percentage of the comparable dimension of the excitatory receptive fields. The non-selective cells are represented by the bins at the right. The average length of the excitatory receptive fields in DL was 20.3° with a standard deviation of 9.5°. The average length of the excitatory receptive fields in DM, MT, and M was 15° with a standard deviation of 7.4°.

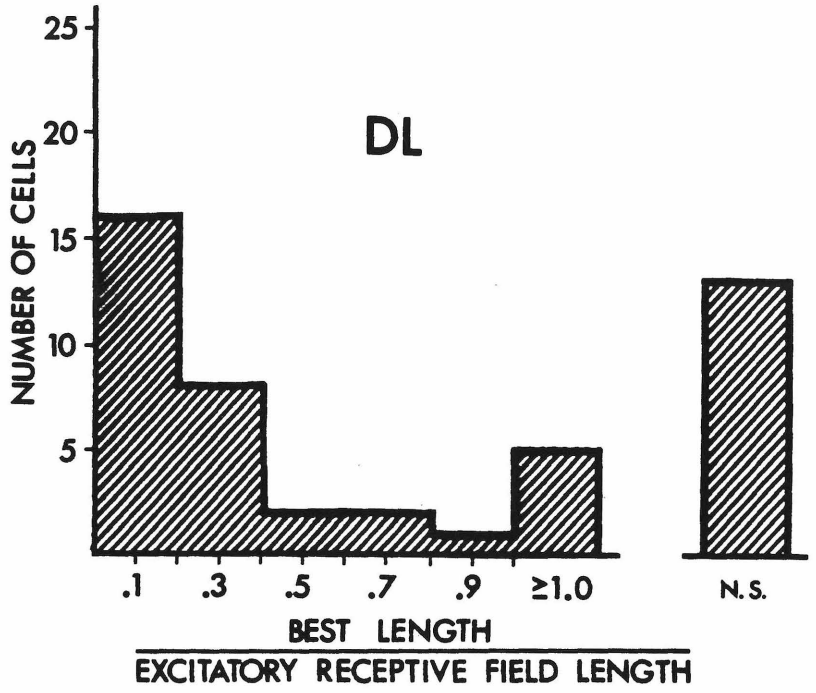
DL
NUMBER OF CELLS
25
20
15
10
5
.1
.3
.5
.7
.9
≥1.0
N.S.
BEST LENGTH
EXCITATORY RECEPTIVE FIELD LENGTH

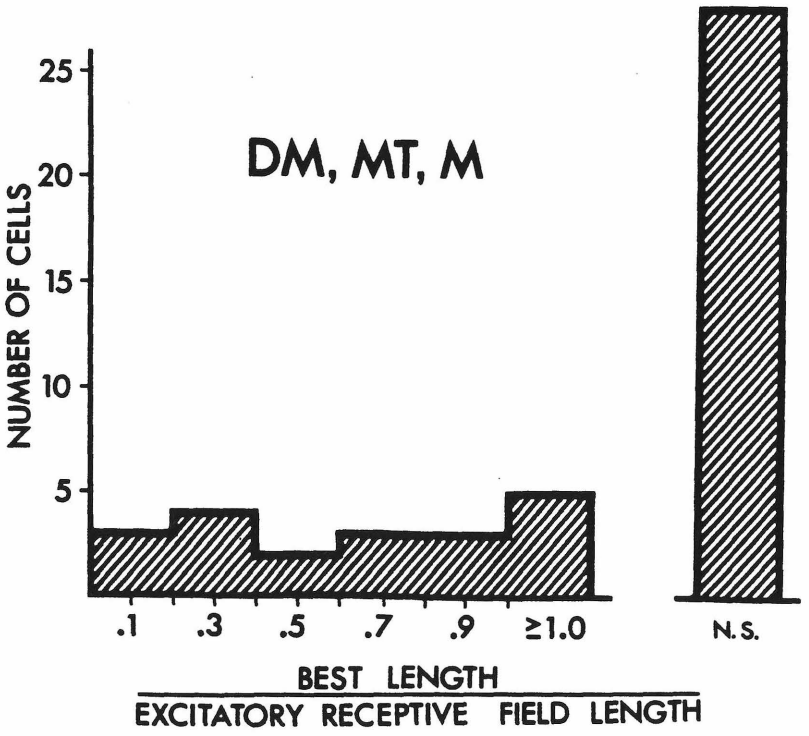
DM, MT, M
NUMBER OF CELLS
25
20
15
10
5
.1
.3
.5
.7
.9
≥1.0
N.S.
BEST LENGTH
EXCITATORY RECEPTIVE FIELD LENGTH

Figure 5. Optimal stimuli derived from the length, width, and spot diameter series. Length is represented in the vertical dimension, and width in the horizontal dimension. The number under each stimulus represents the number of times that the particular stimulus was encountered.

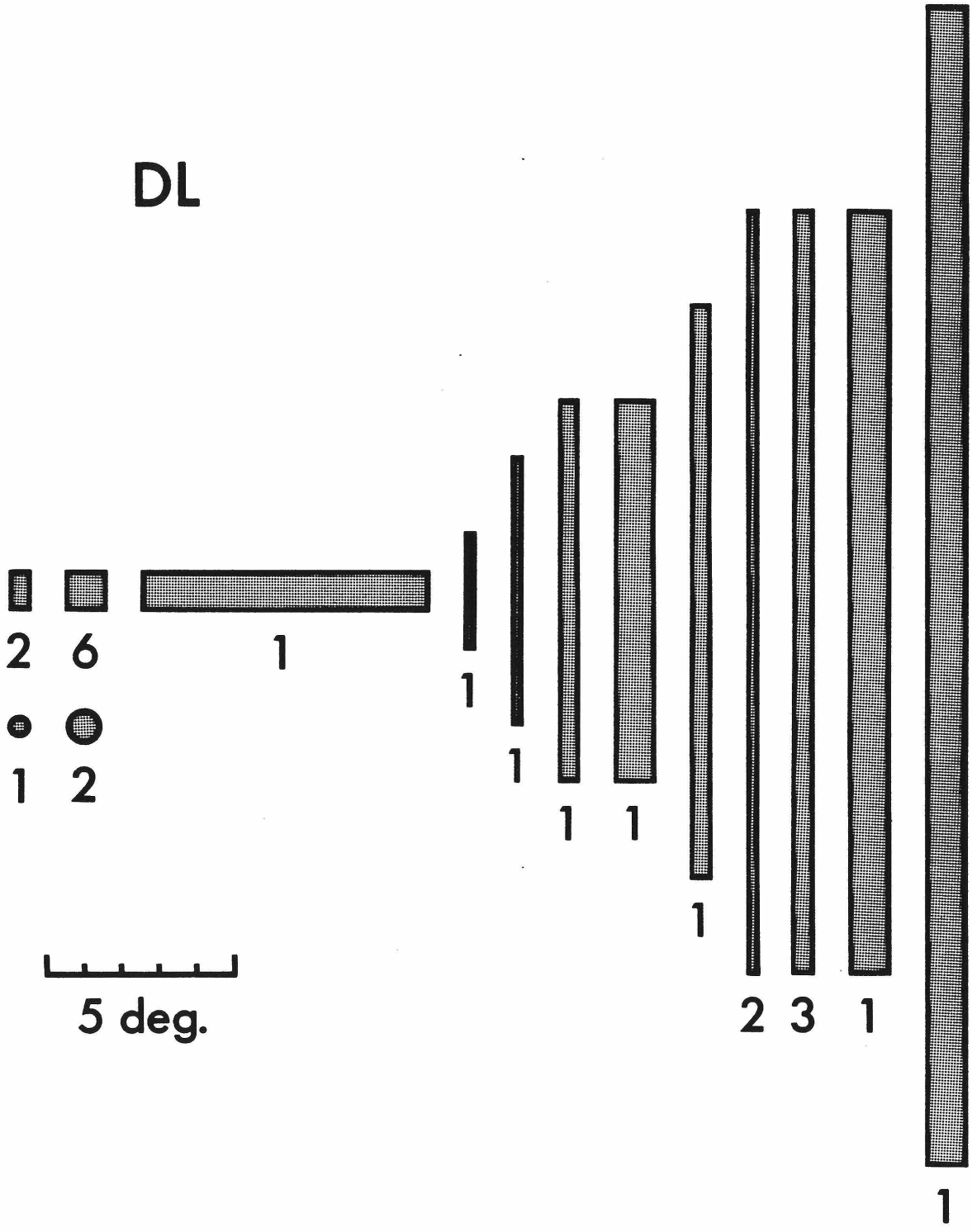

OPTIMAL STIMULUS DIMENSIONS

order hypercomplex pattern of selectivity to sets of orientations 90 degrees apart. The strongest similarities exist between the DL neurons and the neurons of the medial bank of the lateral suprasylvian sulcus in the cat studied by Camarda and Rizzolati (4). There is agreement in every category reported, and a striking similarity between the percentage of dimensionally-selective cells found in the two regions. There have been conflicting reports as to whether the lateral suprasylvian sulcus neurons are orientation selective or not (11, 16, 18). In the owl monkey, virtually all of the extrastriate neurons we tested, including those in DL, were selective for the orientation of a flashed stationary bar.

In summary, a large percentage of DL cells respond selectively to the spatial dimensions of visual stimuli. This selectivity is independent of the contrast, or intensity of the stimulus, and of its position in the excitatory receptive field. These cells show a broad range of preferred dimensions. These results are strongly suggestive that one of the functions of the dorsolateral area is the discrimination of the size of the visual stimulus.

An important question left unresolved by our experiments is that of whether DL neurons respond to retinal image size or to perceived size; specifically, do they exhibit size constancy in the presence of depth cues (9)? In either case, the spatial selectivity of these cells likely contributes to the perception of size, and may contribute to the determination of size constancy.

The dimensional selectivity of DL neurons also implicates DL in the perception of shape or form. This is consistent with the other observations about this area: the aforementioned expanded representation of the central visual field and the observation that DL is a main source of input to the inferotemporal cortex (17), a region which has been strongly implicated in the analysis of complex visual stimuli and the learning of visual form discrimination (7, 8).

Legend for Table 1

L/D, fires to light-on-dark stimuli; D/L, fires to dark-on-light stimuli; Dir. sel., directionally selective; Orien. sel., orientation selective; Sus./Trans., Sustained or transient response; Opt. stim./Excitat. RF, optimal stimulus as a fraction of the excitatory receptive field dimension.

*The receptive field of an event detector colliculus cell had a small central excitatory region with a larger inhibitory surround, making it difficult to determine whether response was independent of excitatory receptive field position and what relation there was between the optimal stimulus size and the excitatory receptive field size.

**In categories 2 and 3, the optimal stimulus was much smaller than the excitatory receptive field. In category 4, the optimal stimulus was the same length as the receptive field.

Table 1

Author	Animal	Structure	Cell type	% of cells	L/D	D/L	Dir. sel.	Orien. sel.	Independently tuned in both dimensions	Independent of stimulus position	Sus./ Trans.	Opt. stim. Excitat. RF
Maturana et al.	frog	optic nerve and tectum	convex edge detectors	not rep.	no	yes	not rep.	not rep.	no	no	sus.	1°-3°/3°-5°
Hubel and Wiesel	cat	area 19	higher order hypercom.	10% (11/109)	yes	yes	yes	yes	yes	yes	trans.	25°/much larger stim.
Levick	rabbit	vis. strk. ret. gang. cells	local edge detectors	19% (30/154)	yes	yes	no	no	no	no	trans.	-1°/.5°-2°
Schiller and Koerner	macaque monkey	superfic. layers sup. coll.	event detectors	42% (102/243)	yes	yes	no	no	no	*	trans.	*
Cleland and Levick	cat	ret. gang. cells	local edge detectors	5% (45/960)	yes	yes	no	no	no	no	trans.	.2°-.6°/.5°-3°
Camarda and Rizzolati	cat	med. bank lateral suprasyl.	categories 2,3,4	69% (66/95)	yes	yes	yes	not rep.	not rep.	yes	trans.	**
Chow et al.	rabbit	temporal cortex	dark spot cells	38% (29/96)	no	yes	no	no	no	yes	sus.	1°-2°/10°-20°
Chow et al.	rabbit	temporal cortex	dark bar cells	9% (9/96)	no	yes	no	no	yes	yes	trans.	"narrow bar/ 10°-20°
Baizer et al.	macaque monkey	area 18	spot cells	11% (26/238)	yes	not rep.	no	no	no	no	not rep.	"stim. much smaller than RF
Petersen et al.	owl	DL	dimen.-sel. cells	see text	yes	yes	yes	yes	yes	yes	trans.	see text

REFERENCES

1. Allman, J. M. Evolution of the visual system in the early primates. In: Progress in Psychobiology and Physiological Psychology, edited by J. M. Sprague and A. N. Epstein. New York: Academic Press, 1977, Vol. 7, pp. 1-53.
2. Baizer, J. S., Robinson, D. L. and Dow, B. M. Visual responses of Area 18 neurons in awake, behaving monkey. J. Neurophysiol. **40:** 1024-1037, 1977
3. Baker, J. F., Petersen, S. E., Newsome, W. T. and Allman, J. M. Visual response properties of neurons in four extrastriate visual areas of the owl monkey (Aotus trivirgatus): a quantitative comparison of medial, dorsomedial, dorsolateral and middle temporal areas. J. Neurophysiol. **45:** 397-416, 1981.
4. Camarda, R. and Rizzolatti, G. Visual receptive fields in the lateral suprasylvian area (Clare-Bishop area) of the cat. Brain Res. **101:** 427-443, 1976.
5. Chow, K. L., Douville, A., Mascetti, G. and Grobstein, P. Receptive field characteristics of neurons in a visual area of rabbit temporal cortex. J. Comp. Neurol. **171:** 135-146, 1976.
6. Cleland, P. G. and Levick, W. R. Properties of rarely encountered types of retinal ganglion cells in the cat's retina and an overall classification. J. Physiol. London **240:** 457-492, 1974.
7. Gross, C. G. Visual functions of inferotemporal cortex. In: Handbook of Sensory Physiology, Vol. VII/3B, edited by R. Jung. Berlin: Springer, 1973, pp. 451-482.
8. Gross, C. G., Bruce, C. J., Desimone, R., Fleming, J. and Gattas, R. Three visual areas of the temporal lobe. In: Multiple Cortical Areas, edited by C. N. Woolsey. Englewood Cliffs, New Jersey: Humana, in press.
9. Holway, A. F. and Boring, G. G. Determinants of apparent visual size with distance variant. Am. J. Psychol. **54:** 21-37, 1941.

10. Hubel, D. H. and Wiesel, T. N. Receptive fields and functional architecture in two non-striate visual areas (18 and 19) of the cat. J. Neurophysiol. **28:** 229-289, 1965.

11. Hubel, D. H. and Wiesel, T. N. Visual area of the lateral suprasylvian gyrus (Clare-Bishop area) of the cat. J. Physiol., London **202:** 251-260, 1969.

12. Levick, W. R. Receptive fields and trigger features of ganglion cells in the visual streak of the rabbit's retina. J. Physiol., London **188:** 285-307, 1967.

13. Maturana, H. R., Lettvin, J. Y., McCullough, W. S. and Pitts, W. H. Anatomy and physiology of vision in the frog (Rana pipiens). J. gen. Physiol., Suppl. 2, **43:** 129-176, 1960.

14. Pollard, J. H. A Handbook of Numerical and Statistical Techniques. Cambridge: Cambridge University Press, 1977.

15. Schiller, P. H. and Koerner, F. Discharge characteristics of single units in superior colliculus of the alert rhesus monkey. J. Neurophysiol. **34:** 920-936, 1971.

16. Spear, P. D. and Baumann, T. P. Receptive-field characteristics of single neurons in lateral suprasylvian visual area of the cat. J. Neurophysiol. **38:** 1403-1420, 1975.

17. Weller, R. E. and Kaas, J. H. Connections of the dorsolateral visual area (DL) of extrastriate visual cortex of the owl monkey (Aotus trivirgatus). Soc. Neurosci. Abstr. **6:** 580, 1980.

18. Wright, M. J. Visual receptive fields of cells in a cortical area remote from the striate cortex of the cat. Nature, London **223:** 973-975, 1969.

Chapter 3

DIRECTION-SPECIFIC ADAPTATION IN AREA MT OF OWL MONKEY

INTRODUCTION

The motion aftereffect, or "waterfall illusion", is a well-known perceptual phenomenon. After prolonged exposure to motion in a certain direction, such as prolonged staring at a waterfall, stationary objects appear to be moving in the opposite direction. This change in perception of motion may reflect short term changes in neural populations. The visual cortical area MT, because of a high percentage of cells that are selective for the direction of motion, has been suggested to be implicated in motion perception (3, see Chapter 1). In this chapter, neurons in MT are reported which exhibit changes in responsiveness following prolonged exposure to visual stimuli moving in certain directions. When adapting MT neurons in the preferred direction of motion, responses to bars moving in the preferred direction are suppressed; when adapting opposite to the preferred direction, responses to identical bars are enhanced.

The middle temporal area (MT) of the owl monkey is a well-defined region of the temporal lobe that contains a high percentage of directional cells (2, see Chapter 1, 29). This area can be further characterized as a heavily-myelinated striate-receptive region which is coextensive with an orderly map of the visual hemifield (2). Homologies of MT have been documented in several primate species (see Chapter 1, homologies). The directional cells of MT respond well to movement of a visual stimulus in a preferred direction, and poorly to stimuli moving in other directions, with stimuli moving in the direction 180° opposite least effective or inhibitory. In the owl monkey most of the directional cells respond to many types of stimuli (spots, bars, and random dot fields of different sizes and velocities); thus, the direction of movement seems to be an important aspect of a visual stimulus to most MT neurons.

The work of Scott and Milligan (18) suggests that monkeys "see" motion after-effects similar to human aftereffects. Many students of perception have quantitatively explored a related effect in humans. In experiments with moving gratings (20),

and fields of random dots (11), Sekuler and colleagues have shown that adaptation in a certain direction raises the threshold of visibility for similar stimuli moving in the same direction. They have termed this phenomenon direction-specific adaptation. Also, the perceived direction of a moving stimulus is displaced away from the adapted direction for nearby directions of movement (10).

METHODS

Neurons from MT and surrounding cortex were recorded in four chronically-prepared owl monkeys. Recording techniques were similar to those used in Chapters 1 and 2 (3), except that the stimuli were presented on a TV screen by computer-controlled hardware rather than projected on a tangent screen. The TV screen was placed either 28.5 or 57 cm away from the animal so that the 40 cm by 30 cm screen subtended either 40 by 30 or 80 by 60° of the visual field.

A neuron's preferred direction of movement was determined using a series of bar stimuli swept through the receptive field in 12 different directions. The directions were pseudorandomly interleaved and presented five times each. The bar was usually oriented orthogonally to the direction of movement, and was of a length, width, and velocity qualitatively determined to elicit a good response from the neuron.

The cell was then tested for direction-specific adaptation as shown in Fig. 1. A 20 sec adaptation period of random visual noise (dot size = 0.2 cm, 50% density) was presented moving in the preferred direction, 180° opposite to the preferred direction, or as a stationary field. Each adaptation period was followed by a bar sweeping through the receptive field in the best or opposite direction. The test therefore consisted of six possible conditions: three adaptation fields paired with either of two bar stimulus conditions. In an adaptation test series, each of the six conditions was presented five times in a pseudorandomly interleaved sequence. The stationary noise

Figure 1. The left half of Figure 1 is a diagrammatic representation of an adaptation series. A period of adaptation of stationary noise, or noise moving in either the best or opposite directions was followed by a bar stimulus moving in the best or opposite direction. These six conditions were pseudorandomly interleaved, and presented five times each. The right half of the figure shows an example of an adaptation series. Notice that the response is strongest after adaptation in the opposite direction, and weakest after adaptation in the best direction.

RANDOM DOT ADAPTATION FIELD:

FOLLOWED BY BAR STIMULUS IN:

BAXX15DA.03

23. 5.

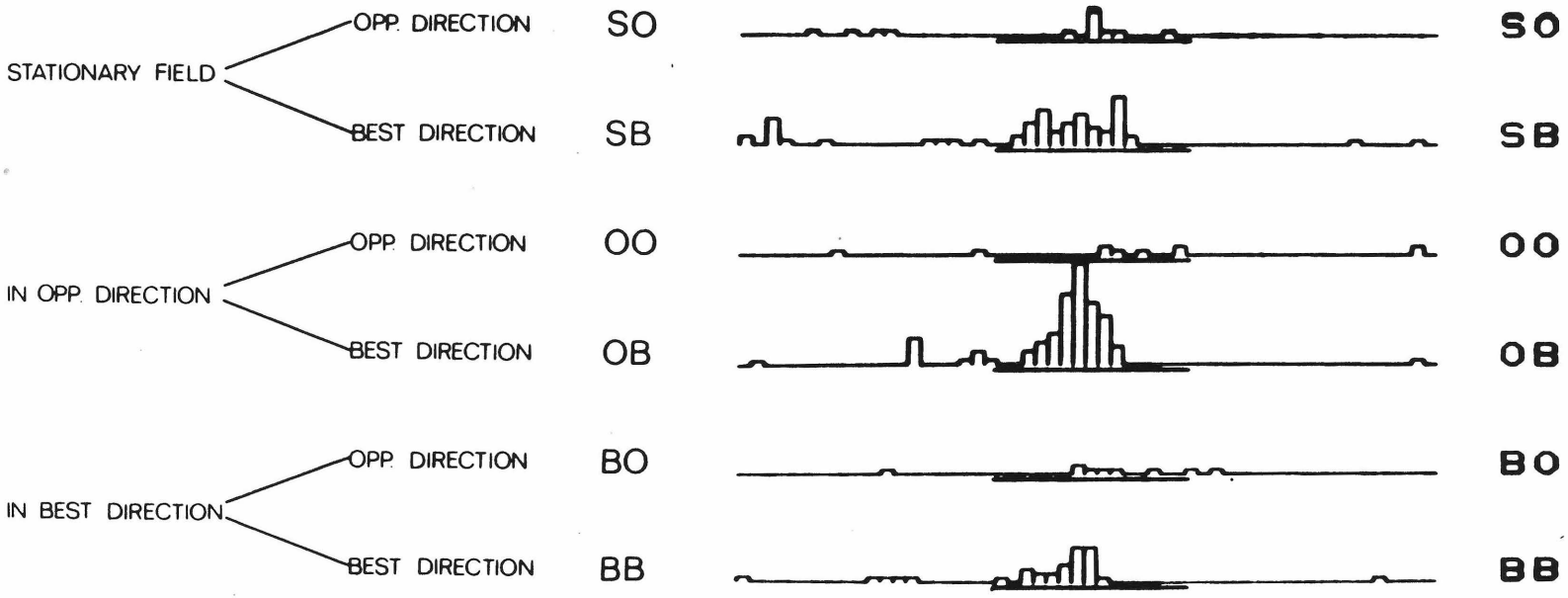

conditions (SB, SO) were used as control conditions to compare changes in responsiveness following adaptation in the best and opposite directions.

RESULTS

We saw strong adaptation effects in most of the directional cells in MT. An online display of an adaptation series is shown in Fig. 1B. In three of the test conditions, SB, OB, and BB, identical bars are moved through the receptive field in the same direction, but the response of the neurons to the bars is affected in a systematic way by the preceding adaptation period. Adaptation in the preferred direction of movement suppressed the response to the bar in the best direction, while adaptation in the opposite direction enhanced the response to the bar in the best direction. The responses to bars in the opposite direction (SO, OO, BO) were generally much weaker, and any changes in their responsiveness was unsystematic.

To compare populations of cells, an adaptation index was computed using the formula:

AI = % enhancement after adaptation in the opposite direction (OB/SB-1) +

% suppression after adaptation in the best direction (1-BB/SB) =

(OB-BB)/SB

The distribution of adaptation indices for 38 directional cells is shown in Fig. 2A. A cell was considered directional if it fired three times as well to a stimulus in the preferred direction than to stimuli in directions 120, 150, or 180° opposite. 61% of the cells studied were directional by this stringent criterion. In a previous study (3), 66% of MT cells were found to meet this criterion. 70% of direction cells had indices higher than 20, 38% higher than 40. The mean adaptation index for direction cells was 36.5 with approximately equal contributions from enhancement (mean = 18.7) and suppression (mean = 17.9) effects. A distribution of the much weaker adaptation effects for nondirectional cells from MT and surrounding cortex is

Figure 2. The distributions of adaptation indices for directional (top) and non-directional (bottom) cells. The adaptation index was calculated by adding the % enhancement after adaptation in the opposite direction to the % suppression after adaptation in the best direction. The adaptation indices for direction cells are generally high, while those for the nondirection cells tend to congregate near zero. The differences between these distributions are statistically significant at the 0.001 level.

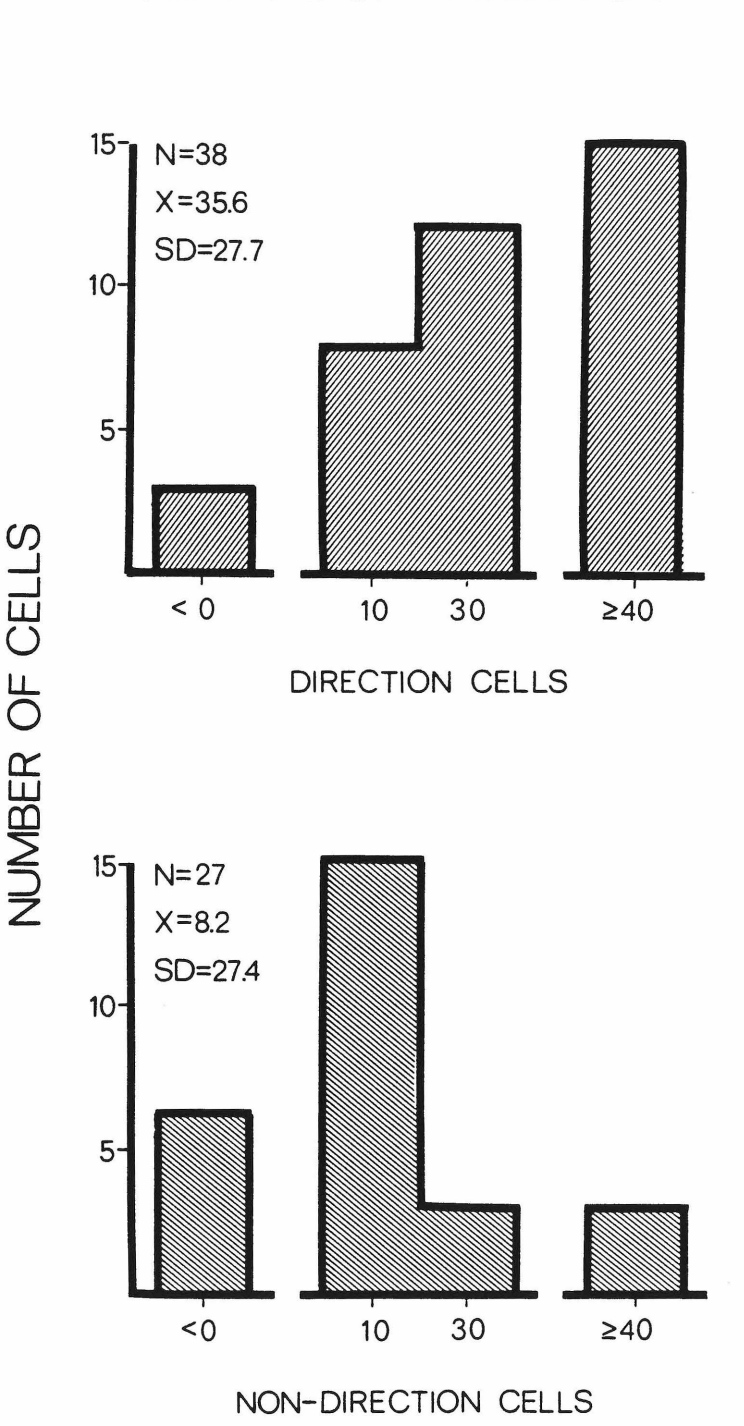
ADAPTATION INDEX FOR:
NUMBER OF CELLS
15
10
5
N=38
X=35.6
SD=27.7
< 0
10
30
≥40
DIRECTION CELLS
15
10
5
N=27
X=8.2
SD=27.4
<0
10
30
≥40
NON-DIRECTION CELLS
A.I. = % ENH. AFTER OPP. + % SUP. AFTER BEST

shown in Fig. 2B. 80% of the nondirectional cells' indices were lower than 20 (mean = 8.1). The differences between these populations were very significant ($t = 3.58$, $p < 0.005$).

Direction cells which exhibited direction-specific adaptation effects were intermixed with nondirection cells that did not show the effect. An example of an oblique penetration is shown in Fig. 3. In this penetration, complete direction preference and adaptation information was collected for eight cells. Five of these cells were clearly directional and had clear adaptation effects. The three nondirectional cells showed little systematic change following the adaptation stimuli.

Although most MT cells respond well to a field of scattered (10% density) 1° spots (3), the finer-grained, higher-density (50%) texture of the noise adaptation field produced by the TV system rarely (5/38) evoked strong responses from directional neurons, and in only one case was this response comparable to the best response to a moving bar. Most often the neurons responded weakly to movement of noise in the best direction, with very weak or no response to either the stationary noise field or the field moving in the opposite direction. A strong response to the adaptation field was not necessary to produce a strong adaptation effect. In the example in Fig. 1B, no response above spontaneous was observed to any of the adaptation stimuli.

Early this century Wohlgemuth reported that repeated presentations of the waterfall illusions in alternating directions of adaptation caused a weakening of the effect over time (27). Although our paradigm tests for direction-specific adaptation rather than for the waterfall illusion, a small progressive decrement of the median adaptation index is suggested by the data shown in Fig. 4.

DISCUSSION

A great deal of psychophysical evidence suggests that there are at least two separate sets of functional pathways in the mammalian visual system. One of these

Figure 3. A display of adaptation effects for eight cells from the same penetration. The polar plot of a cell's directionality is shown in the left hand column, the adaptation index next to the polar plot and the appropriate histograms in the succeeding three columns. For cells with strong directional preferences, such as BAXX21A, C, F, G, and I, the adaptation indices are high, and the histograms reflect this effect. For those cells which are without directional preference E, H, and J, the adaptation indices are uniformly low.

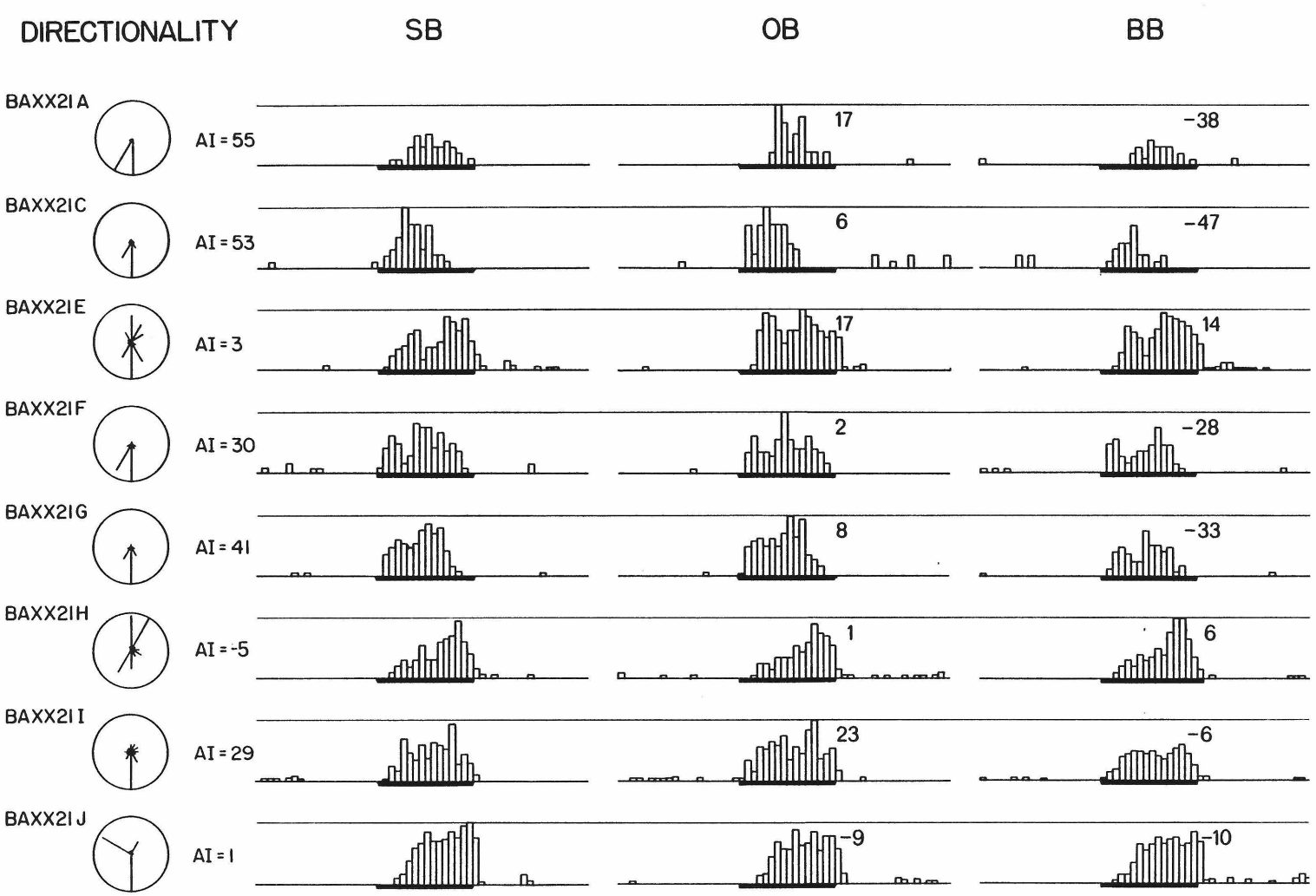
DIRECTIONALITY
SB
OB
BB
BAXX21A
AI = 55
17
-38
BAXX21C
AI = 53
6
-47
BAXX21E
AI = 3
17
14
BAXX21F
AI = 30
2
-28
BAXX21G
AI = 41
8
-33
BAXX21H
AI = -5
1
6
BAXX21I
AI = 29
23
-6
BAXX21J
AI = 1
-9
-10

Figure 4. A plot of the median adaptation index for each run. Wohlgemuth (27) reported a similar run-by-run decrement for repeated presentations of the waterfall illusion in opposing directions.

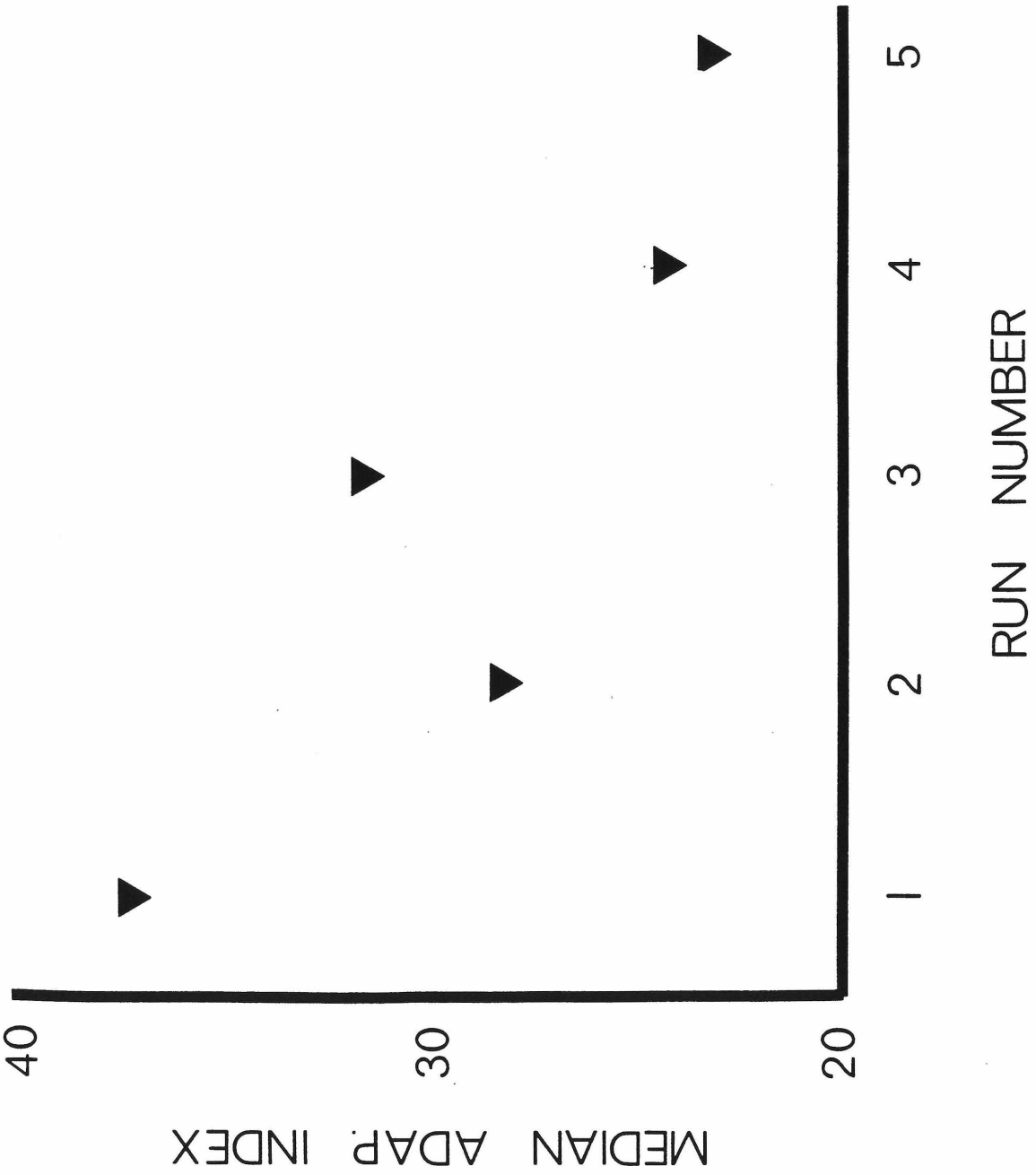
MEDIAN ADAP INDEX
40
30
20
1
2
3
4
5
RUN NUMBER

pathways is more sensitive to the form, or pattern of a visual stimulus, and the other is more concerned with the motion of a stimulus. Sekuler and Levinson reported that there were separate thresholds for the detection of motion of a grating and for the detection of the pattern of the grating itself (11, 19). In a separate set of experiments, they showed that when using a "pattern criterion" after adaptation to a grating, no direction-specific adaptation was reported by the observer (19). Further, a threshold elevation for motion was shown for the direction opposite to the adapted direction when gratings were used as the stimuli, but was not seen when random dot stimuli were employed (11, 20). This and other evidence led to the conclusion that in grating adaptation there were both form- or orientation-specific, and direction-specific mechanisms present, but in the random dot experiments, the direction-specific mechanisms played a greater role.

To dissociate the adaptation due to form, and the adaptation due to direction, perhaps a psychophysical paradigm similar to the one employed in our physiological experiments could be used. Using random dots for adaptation, and bars or gratings for test stimuli may well avoid the confounding influence of form adaptation of either dots or gratings on the direction-specific adaptation.

There is also growing neurobiological evidence for the existence of parallel processing pathways in the visual system. There are several efferent pathways from V-I in the owl monkey. One of these pathways originates in the neurons of the stria of Gennari and the giant meynert cells at the boundary of layers 5 and 6 (25). This pathway projects to MT which in turn projects to most of the known visual areas and regions. A second set of major connections ascends from neurons in layers 2 and 3 of V-I to V-II to DL to IT (12, 13, 25, 26). Evidence from the macaque monkey suggests that these two paths have relatively separate inputs from different layers of the LGN. The magnocellular layers, which have a preponderance of broad-band Y-type cells project mainly onto the Gennari-MT pathway through layer IVc alpha, while the

V-II-DL pathway gets input mainly from X-like cells in the parvo-cellular layers of the LGN, which project to layers 2 and 3 through layer IVc beta (8).

Neurophysiological data confirm that these two pathways contribute to different aspects of visual perception. In area DL, 70% of the neurons are selective for the spatial dimensions (length and width) of visual stimuli (see Chapter 2). DL also has the most expanded representation of the central visual field of all the topographically arranged areas thus far studied in the owl monkey (1), and central vision is where the most acute recognition of form takes place. IT in the macaque appears to contribute to the analysis of complex visual stimuli and the learning of visual form discriminations (6, 7). The specializations of the V-II-DL-IT pathway—discrimination of spatial dimensions, complex stimuli, and the learning of form discrimination—deal with the form of the stimulus.

The MT pathway conversely appears to be more interested in the motion of a stimulus. This pathway is characterized by the high percentage of directional cells found in layer IV-B (the stria of Gennari) in the macaque (5), and the high percentage of directional cells in MT of owl monkey (3, 29). The tuning of MT cells to direction of motion of random dots is strikingly similar to the tuning of the elevation of threshold after direction specific adaptation to random dots in humans (3, 11) (Fig. 5). The direction-specific adaptability of MT cells suggests more strongly that MT contributes to the perception of motion. It must be noted however that we have not tested for direction-specific adaptation in other regions of cortex, so we cannot say that these effects are completely localized to MT. It is also quite likely that either or both of these pathways must contribute to other aspects of visual perception, such as color vision, depth perception, etc., and that other pathways may well contribute to the perception of form and motion.

Barlow (4) previously reported direction cells in the retina of the rabbit which responded strongly to a prolonged stimulus moving in one direction. After the

Figure 5. On the left is a polar plot of direction-specific adaptation in a human subject from Levinson and Sekuler (10). The adapting stimulus was a field of random dots moving in the direction indicated by the arrow. The distance from the center of the polar plot is the log elevation in detection threshold for various directions of moving test dots. On the right is a polar plot of the response of an MT neuron to a field of random dots moving in different directions. The distance from the center of the plot is the average response in spikes per second. The tuning of directional selectivity for this neuron is almost exactly the mean for the population of MT neurons tested with random dots (53, see Chapter I).

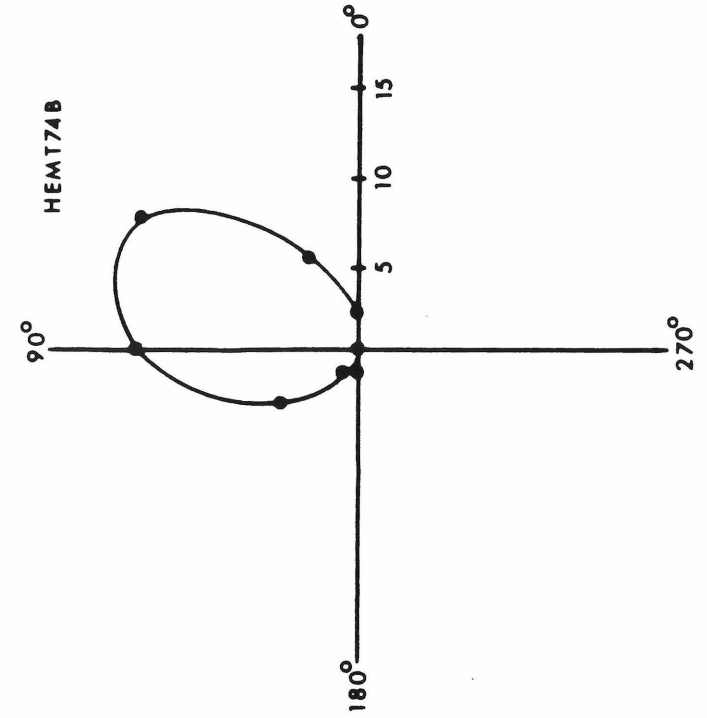

MT NEURON

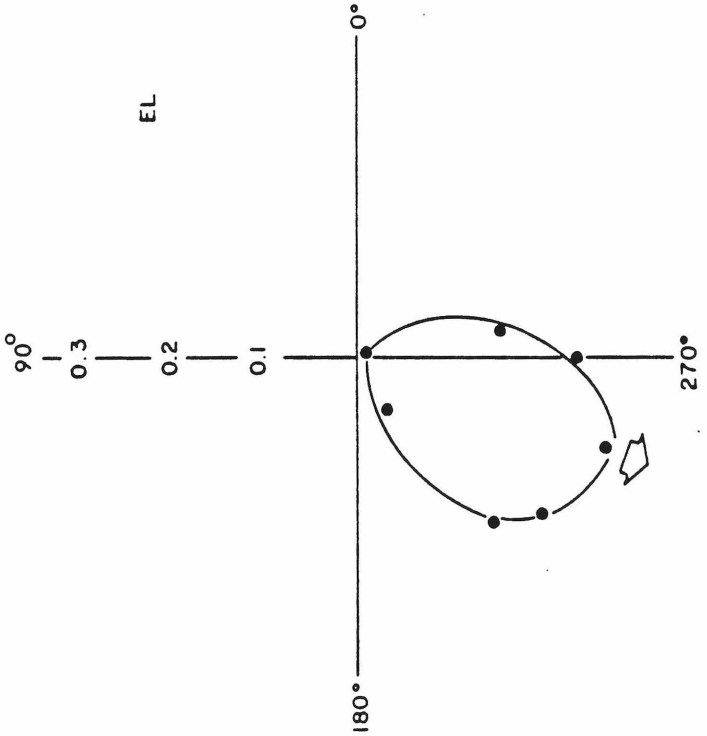

MOTION AFTER EFFECT

prolonged stimulation, the cells showed a suppression of spontaneous firing for a period of time appropriate to the waterfall illusion. Similar effects have been reported in the striate cortex of the cat by Vautin and Berkeley (24). The cat striate cells exhibited habituation effects which were consistent with the decay of visual aftereffects. These cells showed some direction specificity, and a small amount of adaptation in the non-preferred direction consistent with the fact that they used gratings and bars as adaptation stimuli, and thus could have been adapting the cells for orientation as well. Movshon et al., in a recent report (17), demonstrated that adaptation effects for contrast sensitivity were present at the level of the striate cortex but were absent at the level of the LGN. In cat striate cortex, the directional cells were also more affected by adaptation. Fatiguable cells such as these could provide input to the adaptable MT neurons. The enhancement of MT cells could be the result of the habituation of an inhibitory input tuned to the direction opposite the preferred direction of movement. However, the adaptation effects of MT neurons cannot be explained by fatiguing at the level of MT, since in the MT neurons, the adaptation stimulus rarely fires the cell at a high rate.

The suppression of a bar response after adaptation is consistent with the suppression of detectability of gratings reported psychophysically by Sekuler and colleagues. However, the enhancement effect evident in MT neurons was not directly predicted by previous psychophysical or neurophysiological reports. Some models forwarded by psychophysicists to explain the motion aftereffect and direction-specific adaptation include comparisons between direction-specific channels tuned for opposing directions of movement (16, 22), or distributions of activity of several direction-specific channels (15). One of these models predicts a facilitation of response similar to the enhancement effect seen in MT cells (16).

The response of MT directional neurons is contingent on the degree of difference between a stimulus' motion and the motion of the preceding period of

adaptation. If a bar stimulus moves in the same direction as (i.e., is similar with respect to direction to) the adaptation stimulus, the subsequent response is weakest. If a bar is most different, moving in the opposite direction, then the response is strongest. With the intermediate condition of bar movement following stationary adaptation the bar elicits a response of intermediate strength.

REFERENCES

1. Allman, J.M. Evolution of the visual system in the early primates. In: Progress in Psychobiology and Physiological Psychology, edited by J. M. Sprague and A. N. Epstein. New York: Academic Press, 1977, Vol. 7, pp. 1-53.
2. Allman, J. M. and Kaas, J. H. A representation of the visual field in the caudal third of the middle temporal gyrus of the owl monkey (Aotus trivirgatus). Brain Res. **31:** 84-105, 1971.
3. Baker, J. F., Petersen, S. E., Newsome, W. T. and Allman, J. M. Visual response properties of neurons in four extrastriate visual areas of the owl monkey (Aotus trivirgatus): a quantitative comparison of medial, dorsomedial, dorsolateral and middle temporal areas. J. Neurophysiol. **45:** 397-416, 1981.
4. Barlow, H. B. and Hill, R. M. Evidence for a physiological explanation of the waterfall phenomenon and figural aftereffects. Nature **200:** 1345-1347, 1963.
5. Dow, B. M. Functional classes of cells and their laminar distribution in monkey visual cortex. J. Neurophysiol. **37:** 927-946, 1974.
6. Gross, C. G. Visual functions of inferotemporal cortex. In: Handbook of Sensory Physiology, VII/3 B, edited by R. Jung. Berlin: Springer, 1973, pp. 451-482.
7. Gross, C. G., Bruce, C. J., Desimone, R., Fleming, J. and Gattas, R. Three visual areas of the temporal lobe. In: Multiple Cortical Areas, edited by C. N. Woolsey. Englewood Cliffs, NJ: Humana. In press.
8. Hubel, D. H. and Wiesel, T. N. Laminar and columnar distribution of geniculo-cortical fibers in the macaque monkey. J. Comp. Neurol. **146:** 421-450, 1972.
9. Kandel, E. The Cellular Basis of Behavior. San Francisco: Freeman Press, 1976.
10. Levinson, E. and Sekuler, R. Adaptation alters perceived direction of motion. Vis. Res. **16:** 779-781, 1976.

11. Levinson, E. and Sekuler, R. A two-dimensional analysis of direction-specific adaptation. Vis. Res. **20:** 103-107, 1980.

12. Lund, J. S., Lund, R. D., Hendrickson, A. E., Bunt, A. H. and Fuchs, A. F. The origin of efferent pathways from the primary visual cortex, area 17, of the macaque monkey as shown by retrograde transport of horseradish peroxidase. J. Comp. Neurol. **164:** 287-304, 1976.

13. Lund, J. S., Henry, G. H., MacQueen, C. L. and Harvey, A. R. Anatomical organization of the primary visual cortex (area 17) of the cat. A comparison with area 17 of the macaque monkey. J. Comp. Neurol. **184:** 599-618, 1979.

14. Marr, D. and Ullman, S. Directional selectivity and its use in early visual processing. Proc. R. Soc. Lond., B **211:** 151-180, 1981.

15. Mather, G. The movement aftereffect and a distribution-shift model for coding the direction of visual movement. Perception **9:** 379-392, 1980.

16. Moulden, B. and Mather, G. In defense of a ratio model for movement detection at threshold. Quart. J. Exptl. Psychol. **30:** 505-520, 1978.

17. Movshon, J. A., Bonds, A. B. and Lennie, P. Pattern adaptation in striate cortical neurons. ARVO (abst.), 1980, p. 193.

18. Scott, T. R. and Milligan, W. L. The psychophysical study of visual motion aftereffect rate in monkeys. In: Animal Psychophysics, edited by W. C. Stebbins. New York: Appleton-Century-Crofts, 1970, pp. 341-361.

19. Sekuler, R. Visual motion perception. Handbook of Perception V: 387-433, 1975.

20. Sekuler, R. and Ganz, L. Aftereffect of seen motion with a stabilized retinal image. Science **139:** 419-420, 1963.

21. Sekuler, R. and Levinson, E. The perception of moving targets. Sci. Am. **236:** 60-73, 1977.

22. Sutherland, N. S. Figural aftereffects and apparent size. Quart. J. Exptl. Psychol. **13:** 222-228, 1961.

23. Thompson R. F. and Glanzman, D. L. Neural and behavioral mechanisms of habituation and sensitization. In: Habituation, edited by T. J. Tighe and P. H. Leaton. Hillsdale, N.J.: Erlbaum, 1976, pp. 49-93.

24. Vautin, R. G. and Berkeley, M. A. Responses of single cells in cat visual cortex to prolonged stimulus movement: neural correlates of visual aftereffects. J. Neurophysiol. **40:** 1051-1065, 1977.

25. Weller, R. E. and Kaas, J. H. Cortical and subcortical connections of visual cortex in primates. In: Multiple Cortical Areas, edited by C. N. Woolsey. Englewood Cliffs, N.J.: Humana. In press.

26. Weller, R. E. and Kaas, J. H. Connections of the dorsolateral visual area (DL) of extrastriate visual cortex of the owl monkey (Aotus trivirgatus). Soc. Neurosci. Abstr. **6:** 580, 1980.

27. Wohlgemuth, A. On the aftereffect of seen movement. Brit. J. Psychol. (Mongr. Suppl.) **1:** 1911.

28. Wurtz, R. H., Goldberg, M. E. and Robinson, D. L. Behavioral modulation of visual responses in the monkey: stimulus selection for attention and movement. Prog.. Psychobiol. Phys. Psych. **9:** 43-83, 1980.

29. Zeki, S. M. The response properties of cells in the middle temporal area (area MT) of owl monkey visual cortex. Proc. R. Soc. London Ser. B **207:** 239-248, 1980.